Effects of N source concentration and NH_4^+/NO_3^- ratio on phenylethanoid glycoside pattern in tissue cultures of *Plantago lanceolata* L.: A metabolomics driven full-factorial experiment with LC–ESI–MS^3

Sándor Gonda[a*],Attila Kiss-Szikszai[b], Zsolt Szűcs[a], Csaba Máthé[a], Gábor Vasas[a]

Phytochemistry
Volume 106, October 2014, Pages 44–54

[a] University of Debrecen, Department of Botany, Division of Pharmacognosy, Egyetem tér 1, H-4010 Debrecen, Hungary
[b] University of Debrecen, Department of Organic Chemistry, Egyetem tér 1, H-4010 Debrecen, Hungary
*: gonda.sandor@science.unideb.hu, gondasandor@gmail.com

Highlights

The metabolome response to NH_4^+/NO_3^- ratio and N source was shown to be non-linear.

Compared to Murashige Skoog medium, high natural product yields were observed.

Simulated OFAT experimental designs led to sub-optimal yields for natural products.

N source concentration is to be optimized before NH_4^+/NO_3^- ratio for high NP yield.

Abstract

Tissue cultures of a medicinal plant, *Plantago lanceolata* L. were screened for phenylethanoid glycosides (PGs) and other natural products (NPs) with LC–ESI–MS^3. The effects of N source concentration and NH_4^+/NO_3^- ratio were evaluated in a full-factorial (FF) experiment. N concentrations of 10, 20, 40 and 60 mM, and NH_4^+/NO_3^- ratios of 0, 0.11, 0.20 and 0.33 (ratio of NH_4^+ in total N source) were tested.

Several peaks could be identified as PGs, of which, 16 could be putatively identified from the MS/MS/MS spectra. N source concentration and NH_4^+/NO_3^- ratio had significant effects on the metabolome, their effects on individual PGs were different despite these metabolites were of the same biosynthethic class. Chief PGs were plantamajoside and acteoside (verbascoside), their highest concentrations were 3.54 ± 0.83% and 1.30 ± 0.40% of dry weight, on media 10(0.33) and 40(0.33), respectively.

NH_4^+/NO_3^- ratio and N source concentration effects were examined on a set of 89 NPs. For most NPs, high increases in abundance were observed compared to Murashige–Skoog medium. Abundances of 42 and 10 NPs were significantly influenced by the N source concentration and the NH_4^+/NO_3^- ratio, respectively. Optimal media for production of different NP clusters were 10(0), 10(0.11) and 40(0.33). Interaction was observed between NH_4^+/NO_3^- ratio and N source concentration for many NPs. It was shown in simulated experiments, that one-factor at a time (OFAT) experimental designs lead to sub-optimal media compositions for production of many NPs, and alternative experimental designs (e.g. FF) should be preferred when optimizing medium N source for optimal yield of NPs. If using OFAT, the N source concentration is to be optimized first, followed by NH_4^+/NO_3^- ratio, as this reduces the likeliness of suboptimal yield results.

InChIKeys

- KFEFLPDKISUVNR-QJEHNBJNSA-N;
- FBSKJMQYURKNSU-UJERWXFOSA-N;
- CSPZDKXXMYZQPO-SUGCTHRDSA-N;
- UHIGZYLCYRQESL-VJWFJHQPSA-N;
- UDHCHDJLZGYDDM-SLZARYJYSA-N;
- ZMYQRHSOVRDQDL-UNCYNJIFSA-N;
- SCMLVRWSBIVDLC-CUDWIMPTSA-N
-

Abbreviations

- Ara, arabinose;
- BAP, benzyl-aminopurine;
- CA, caffeic acid;
- CID, collision induced dissociation;
- 2,4-D, 2,4-dichlorophenoxyacetic acid;
- FF, full factorial;
- GI, growth index;
- Glc, glucose;
- HT, hydroxytyrosol;
- MeCA, methyl-caffeic acid;
- MSM, Murashige Skoog medium;
- NP, natural product;
- OFAT, one factor at a time;
- PC, principal component;
- PCA, principal component analysis;
- pCoumA, para-coumaric acid;
- PG, phenylethanoid glycoside;
- Rha, rhamnose;
- TC, tissue culture;
- TIC, total ion chromatogram
-

Keywords

- Phenylpropanoid glycosides;
- Polyphenolic substances;
- Phenoloid secondary metabolites;
- Data-mining;
- Design of experiments;
- Medicinal plant tissue culture;
- Omics;
- Ammonium;
- Nitrate

1. Introduction

There is an increasing demand for discovery of bioactive natural products (NPs) to obtain lead compounds for development of new pharmaceutical agents and chemicals useful for agriculture and other industries (Harvey, 2008). Many organisms are screened for agents with antibacterial, antifungal or more specific pharmacological actions. The plant kingdom is still one of the main sources of these bioactive lead compounds – the plants feature an unimaginable variability of bioactive NPs. With the recent advances in biotechnology and analytical chemistry, novel sources of NPs are becoming more accessible for screening to the scientific community and industries. The application of the "omics" approach and data-mining also speeds up this field of research significantly (Harvey, 2008).

A promising means for production of different NPs is medicinal plant tissue cultures (TCs). Drugs of complex chemical structure can be produced in plant TCs in an economical way. Since its very beginning, the technique was planned to be used for in vitro optimized production of NPs. Many problems have been solved and several limitations have been recognized in TCs (Collin, 2001). First of all, several factors have been described to influence production of metabolites in TCs of plants. In general, we can state, that every culture condition has some effect on the metabolite biosynthesis and accumulation, acting through effects on the pattern of the expressed genes (Collin, 2001 and Zhao et al., 2005). The pattern and concentration of NPs is usually different from that of the field-grown whole plants (Budzianowska et al., 2004 and Collin, 2001), mainly because the constantly growing cultures remain in an undifferentiated state, and the culture conditions also do not resemble the outdoor environmental conditions: the TCs develop in a sterile, pathogen-free, herbivore-free environment, which lacks the signals that usually trigger synthesis of the metabolites that protect the plant from stressors (Zhao et al., 2005). The availability and concentration of soluble nutrients is also very different. Another significant problem is that intensive growth and intensive secondary metabolite biosynthesis rarely occurs simultaneously (Collin, 2001). The use of auxin hormones that enable the maintainability of TCs – especially 2,4-D – also silences lots of genes (George et al., 2007).

Some of these problems can be partially overcome by techniques aimed at increasing NP production, such as elicitation and immobilization techniques (Collin, 2001). These techniques however require additional instrumentation or the addition of chemically often uncharacterized, expensive (fungal extracts) or environmentally harmful agents (for example, high concentration of transition metal salts) to the medium. Simpler methods include precursor feeding, and manipulation of the medium components (Collin, 2001).

Macronutrient composition also significantly influences both the growth and NP production in TCs. The N-source type and concentration, N/C-source ratio, C-source type and concentration (various mono- and disaccharides can be used), as well as potassium, phosphate, magnesium and many other components have effects on development and NP production in plant TCs. When optimizing a medium composition with respect to N source, the ratio of NH_4^+ and NO_3^-, and the total amount of available N is usually optimized (George et al., 2007).

Phytochemical analysis of TCs is usually accomplished by methods optimized for whole organs, plant drugs. As the NP pattern can be substantially different, only the high-resolution chromatographic methods provide enough specificity to characterize these systems. Very high theoretical plate numbers can be achieved with capillary electrophoresis (CE) techniques, and lots of information can be gathered about the chemical pattern of the TCs with hyphenated techniques, such as liquid chromatography–mass spectrometry (LC–MS), and especially tandem mass spectrometry (LC–MS/MS, LC–MS^n), or

direct NMR spectroscopy of the samples. Usage of these techniques as primary screening methods is becoming primal.

With these techniques, an extremely large amount of data can be obtained about the contained NP mixture. However, the interpretation of these data (abundance of hundreds of NMR signals, or, peak areas of hundreds of separated peaks in LC/MS^n) and the evaluation of the effects of the treatments can be extremely difficult with traditional approaches such as regression models, especially if two or more factors are optimized. Thus, the results are typically data-mined for the visualization, pattern recognition and identification of the phenomena. The approach has some drawbacks – metabolite identification is often referred to as putative as many types of isomeries cannot be resolved, but also has great advantages like a much higher throughput than that of other approaches, being more inexpensive and much more sensitive compared to purification and identification of molecules requiring milligrams of each NP. Testing the effects of culture parameters on the chemical composition of the tissues now starts to include the very promising metabolomic approach, as presented in a recent study (Guarnerio et al., 2012).

These molecules can be lead compounds for pharmaceutical molecule searches as they have many interesting pharmacological effects. Besides their often cited high antioxidant potential, more interesting bioactivities have been described for these water- and alcohol soluble NPs. Several PGs have shown neuroprotective effects. Anti-inflammatory, hepatoprotective and immunomodulating, analgesic and antihypertensive effects (through inhibition of angiotensin-converting enzyme) effects are also described (Fu et al., 2008).

Our selected model plant, *Plantago lanceolata* L. was also shown to contain many phenylethanoid glycosides. In this genus, these molecules are widespread (Beara et al., 2009 and Ronsted et al., 2003). What is more, these molecules are well biosynthesized in tissue culture conditions, as presented by Budzianowska et al. (2004) and Fons et al. (1999). The *P. lanceolata* plant and its relatives have been subjects of many tissue culture studies, a recent review is available in the literature (Fons et al., 2008). The most abundant PGs in *P. lanceolata* calli were found to be acteoside and plantamajoside (plantamajoside), but lacked flavonoids and iridoids (Budzianowska et al., 2004). Some PGs detected from *P. lanceolata* calli (also found in this study) are shown in Fig. 1.

Our main goal was to examine the effects of the N source concentration and the NH_4^+/NO_3^- ratio on the metabolome of a medicinal plant tissue culture, focusing on a medicinally important natural product class, phenylethanoid glycosides, aimed to be identified by LC–MS^3. As a model, *P. lanceolata* tissue cultures were selected for the study. A full-factorial experiment was designed to enable the detection of possible interactions between the N source concentration and the NH_4^+/NO_3^- ratio. We also aimed to compare the performance of the full factorial (FF) experimental design model with that of the most frequently used one factor at a time (OFAT) experimental design.

2. Results and discussion

2.1. Effects of N source on growth of *P. lanceolata* calli

The calli of *P. lanceolata* were cultured on modified Murashige Skoog media with different NH_4^+/NO_3^- ratios and N source concentrations in a full factorial experiment. For experimental design, nomenclature of media and details, please see Section 4.4.

Growth indices on different media ranged from 4.52 ± 0.10 (40(0.33)) to 9.87 ± 3.31 (20(0)). Unsurprisingly, the concentration and composition of the N source influenced the growth of the *P. lanceolata* TC. A more detailed insight was obtained by subjecting all known medium parameters to ANOVA models, with the growth index being the response variable. It was shown, that N source concentration (ranging from 10 to 60 mM) did not significantly alter growth of the calli, while NH_4^+/NO_3^- ratio had a more pronounced effect. Addition of different amounts of NH_4^+ and NO_3^- required counter-ions, which were Na^+ and Cl^-, added in the range 0–41 and 0–16 mM, respectively, to the different media. The amount of these ions was shown to have only insignificant effects on growth of the TC. Higher concentrations of NH_4^+ have led to decreased growth of the tissue cultures. This is in accordance with that described by Budzianowska et al. (2004) and is usually attributed to the direct toxicity of excess NH_4^+ at higher concentrations (George et al., 2007). Examination of the effects on growth was secondary, our main focus was to detect the changes in the metabolome, which will be detailed in the following sections.

2.2. Phenylethanoid glycosides in *P. lanceolata* calli

After a few preliminary tests, calli from media with 10 mM N were selected for the qualitative study. Ten microliters of the concentrated MeOH extract were injected into a semi-preparative HPLC system (Supelco C18 column, 250 mm × 10 mm × 5 μm; gradient was adapted from the LC–MS method described in Section 4.5) for HPLC-UV–Vis measurement. Most of the NPs in the polarity range examined later were found to have the UV–Vis spectrum characteristic to phenylethanoid glycosides, i.e. maxima around 248, 290 and 330 nm were found (Shi et al., 2013). These wavelengths are unaffected by methylation of the aglyca (Shi et al., 2013). The same pattern was found by Budzianowska et al. (2004), who reported lack of other phenolic NP groups in *P. lanceolata* TC.

Negative mode LC–ESI–MS^3 was shown to be a very suitable method for characterization of the NPs from the MeOH extracts of *P. lanceolata* calli. A high number of $[M-H]^-$ peaks were detected in the total ion chromatogram (Fig. 2). Putative identification was carried out using detailed study of the fragmentation patterns of the two authentic standards plantamajoside and acteoside, application to the similar PGs, and consulting the scientific literature. Fragmentation patterns of most PGs also present in these samples are described in Li et al., 2009, Petreska et al., 2011 and Qi et al., 2012 and Shi et al. (2013). For practical reasons and to show the "taxonomy" of the detected molecules and fragments, the abbreviations of the PG subunits (glucose (Glc), caffeic acid (CA), hydroxytyrosol (HT), etc.) will be used to indicate what parts make up a particular fragment: e.g. $[HT\text{-}Glc(Glc)\text{-}CA - H]^-$ is the m/z 639 ion shown in Fig. 3. The NPs that could be putatively identified from the MS^3 fragmentation are shown in Table 1.

Major PGs were shown to be plantamajoside (**18**, $[M-H]^-$: $[HT\text{-}Glc(Glc)\text{-}CA - H]^-$) and acteoside (verbascoside, **27**, $[M-H]^-$: $[HT\text{-}Glc(Rha)\text{-}CA - H]^-$), their retention times and mass spectra were identical with our authentic standards (Fig. 2). Their isomers (**43** for **27** and **37**, **49** for **18**) were also abundant, these can either be isoacteoside and isoplantamajoside, or cis-acteoside and cis-plantamajoside (Li et al., 2009) – cis/trans pairs can appear as separate peaks in HPLC according to Budzianowska et al. (2004), even from solution of purified standards. The fragmentation routes of 18 and **27** were identical to that of acteoside (Li et al., 2009). The proposed fragmentation pattern of plantamajoside is presented in Fig. 3, that of acteoside is presented in Supplementary Fig. 1.

More polar PGs were detected at lower retention times. **8** was putatively identified as a PG bearing an additional glucose (hexose) on plantamajoside, presenting the $[HT\text{-}Glc(Glc,Glc)\text{-}CA - H]^-$

deprotonated molecular ion (m/z 801). In MS^2, it yielded [HT-Glc(Glc)-CA – H]$^-$ ([M−H]$^-$ of **18**), which could be fragmented further, and yielded the same fragments, as **18** (m/z 477 and m/z 315). 19 was putatively identified as lavandulifolioside, showing fragmentation described in Schmidt et al. (2013). The compound was described in *P. lanceolata* leaves, and micropropagated plants, but could not be detected from calli so far (Budzianowska et al., 2004). Proposed fragmentation scheme is available in Supplementary Fig. 2.

Simpler PGs were also found in the calli, as also presented in Budzianowska et al. (2004). **22** and **30** (m/z 477) were putatively identified as desrhamnosyl-acteoside (=calceorioside B) and its isomer. Distinguishment of the suggested deprotonated molecular ion [HT-Glc-CA – H]$^-$ from [HT-Glc-Glc – H]$^-$ (both m/z 477) was done on basis of retention time (polarity in RP-HPLC), and the presence of fragments, that can be linked to CA, and cannot be explained by fragmentation of glucose. The proposed fragmentation scheme of **22** is plotted in Supplementary Fig. 3.

In the higher retention time range, several less polar PGs were detected. Some of them could also be putatively identified, some were found to be methylated PGs. Of these, many had methyl-caffeic acid (MeCA) as a phenylpropanoid aglycon, and this was found to be the case with **59** (leucosceptoside A, [M−H]$^-$: [HT-Glc(Rha)-MeCA – H]$^-$); **53** and **61** ([M−H]$^-$: [HT-Glc(Glc)-MeCA – H]$^-$). The decay routes of these NPs were identical to that described in Kırmızıbekmez et al. (2005). The proposed fragmentation schemes are shown in the Supplementary Fig. 4. The structures of these three NPs were supported by the presence of fragments m/z 491 [HT-Glc-MeCA – H]$^-$ and 315 [HT-Glc – H]$^-$, indicating that it was not the HT aglycon, that carried the methyl group. The fragment ion m/z 477 can be interpreted as [HT-Glc-Glc – H]$^-$ in this case, unlike in most other PGs. Methylated plantamajoside derivates have only been described from *Digitalis* (Jin et al., 2011) so far.

Even less polar, dimethyl- and/or acetylated PGs were also found. **64** was putatively identified as dimethyl-plantamajoside, both aglyca (HT and CA) were found to be methlyated, [M−H]$^-$: [MeHT-Glc(Glc)-MeCA – H]$^-$. The fragmentation pattern fully supports this structure, the most specific fragment was [MeHT-Glc-MeCA – H]$^-$ (m/z 505).

In the case of **71** and **65**, the two, completely identical fragmentation patterns indicated the structure [HT-Glc(Ac)(Rha)Me_2CA – H]$^-$. The CH_3CHO loss from the dimethyl CA aglycon was the main fragmentation route resulting in [MeHT-Glc(Ac)(Rha)-pCoumA – H]$^-$ (m/z 649), by conversion of the CA aglycon into p-coumaric acid (pCoumA). The ion m/z 649 yielded several fragments in MS^3, all supporting the proposed structure. Identification of fragments, and pathways of decay in MS/MS is summarized in Supplementary Fig. 5.

Many unidentified peaks were also detected. These showed characteristic fragments common to the identified PGs. Several of them also showed CH_2CO loss, indicating possible presence of an acetyl group, but most had insufficient fragments to deduce their structures, or the pattern led to conflicting evidence on substituent positions. Identification of these molecules was beyond the scope of our study. As most of the found PGs yielded MS^2 ions between 40 and 70% efficacy (ratio of abundance of main MS^2 ion and [M−H]$^-$), the lack of MS^2 ions was considered to be indicative of a substantially different structure. These molecules could not be identified.

2.3. Effects of N source composition on phenylethanoid glycoside pattern and concentration in *P. lanceolata* calli

2.3.1. Effects of N source composition on phenylethanoid glycoside pattern, and the metabolome as a whole

Of the many peaks found in the set of total ion chromatograms, 89 were selected for a more in-depth study (see Section 4.8. for filtering, and data processing). As the dataset had a high degree of multicollinearity, the scaled, centered abundance data of the 89 NPs were subjected to dimensionality reduction with principle component analysis (PCA). The first three PC scores were visualized in a pseudo-3D plot shown in Fig. 4a. It is visible, that high and low NH_4^+ content media are separated along the axis PC2. The media without NH_4^+ had very similar scores suggesting highly similar metabolome. It can also be seen, that the metabolome response seemed to be non-linear, as no other clear trends can be observed in the PCA plot. In the loading plots (Fig. 4b) it is obvious, that a small group of metabolites is responsible for most of the variance in PC2. We can state that the NP pattern as a whole was indicative of both N source concentration and NH_4^+/NO_3^- ratio.

2.3.2. Effects of N source composition on abundance of individual natural products

As we wanted to evaluate the effects of the treatments on the NPs directly, every metabolite abundance was subjected to ANOVA separately, the N source concentration and the NH_4^+/NO_3^- ratio being the independent variables. The highest abundances of individual NPs were compared to those found on the most frequently used TC medium, MSM (60(0.33)), and the 20(0) medium used for the culturing of *P. lanceolata* calli by Budzianowska et al. (2004). Overall, we can state, that the N source composition had a very significant effect on the abundance of individual NPs: the N source concentration significantly influenced the abundance of 42 metabolites ($p < 0.00011$), while the NH_4^+/NO_3^- ratio significantly altered concentrations of 10 metabolites (of 89 NPs examined) ($p < 0.00011$). These results are summarized in Supplementary Table 1.

If we take a closer look at the abundance gains of individual NPs compared to MSM, 60(0.33) in Supplementary Table 1, it can be observed that the conventional medium was one of the worst for production of NPs. For most NPs, the best media were those containing six times less (10 mM) N source only. Most metabolites were synthesized at highest rate, when the NH_4^+/NO_3^- ratio was kept at 0.33, including the chief compound, plantamajoside. The best medium was therefore 10(0.33) for overall production. But, in case the yield of a specific NP would be the aim to be optimized, the optimal medium can be a very different composition (Supplementary Table 1). In many of the studies regarding the optimization of medium N source for high NP yield and growth, media with lower NH_4^+ content than that in MSM was found to be optimal for the production of secondary metabolites, for example in a study on Echinacea adventitious shoots (Wu et al., 2006). In our case, the 10(0.33) or 10(0) media were the best for production of most of the different NPs (Supplementary Table 1). Despite several of the tested NPs were identified as phenylethanoid glycosides, very different responses to NH_4^+/NO_3^- ratio and N source were detected, as detailed later.

After obtaining the correlation matrix of the scaled and centered matrix of metabolite abundances, and clustering of the metabolites with respect to their relative abundances in calli grown on different media, a heatmap was generated in R (Supplementary Fig. 6). A relatively strong multi-correlation can be observed for most of the metabolites. The clustering of the metabolites resulted in six groups (Fig. 4b, Supplementary Fig. 6), that reacted relatively similarly to different media compositions. Interestingly, the NPs putatively identified as PGs were sporadically spread across the clusters with different response to the treatments.

While the abundance of NPs in clusters 1 and 2 was the highest on 10(0), maximal abundances for NPs in clusters 3, 4 or 5 could be achieved on 10(0.33). As 10 mM N media are substantially different from the reference media, the production of these metabolites could be increased to a high extent

(Supplementary Table 1). In many cases, threshold-like responses were found, that were for example described for anthocyanin production response to N source concentration by Hirasuna et al. (1991) in grape cell-cultures. The NP with the highest abundance in the sample was plantamajoside (**18**) in cluster 4. For **18**, the best yield was obtained on medium 10(0.33), where 3.54 ± 0.83% (dry wt.) content was found. The least content was 1.04 ± 0.63% (dry wt.), found on medium 40(0.11). Interestingly, the metabolite with the second highest abundance fell in a different cluster; both the optimal medium and the response to the treatments was found to be substantially different – as it can be seen by comparing the response surfaces (Fig. 5d and f). Acteoside content varied from 0.54 ± 0.29% (of dry wt.) on 20(0) to 1.30 ± 0.40% on 40(0.33).

2.3.3. Statistical interaction between N source and NH_4^+/NO_3^- ratio

Most of the NPs responded in a non-linear fashion to the combinations of these two factors tested. Responses are plotted as heatmaps for better evaluation possibility of this interaction (Fig. 5). As stated before, there were many response types, despite many NPs were putatively identified as phenylethanoid glycosides. The presence of local maxima and/or minima renders the independent optimization of NH_4^+/NO_3^- ratio and N source concentration impossible.

This statistical interaction means that the response to the N concentration at different levels of the NH_4^+/NO_3^- ratio was different: for example in the case of **27** (Fig. 5f), at 0.33 NH_4^+/NO_3^- ratio, the response to the N concentration showed an optimum curve: the highest abundance was detected at 40 mM N, while at 0 NH_4^+/NO_3^- ratio, a threshold-like response was observed, with low abundance except at 10 mM N. This means that if we would have done the yield optimization for **27** using the one-factor at a time design, we might have ended up in a suboptimal medium composition, as shown later by in silico OFAT optimization studies.

The studies on TCs from *Plantago* spp. almost exclusively used the original MS, supplemented with various hormone concentrations (Fons et al., 2008). A few studies used modified MS, these were either diluted variants (e.g. ½ strength) (Fons et al., 2008), or reduction in some inorganic components were used, as in Mederos et al. (1997). The effects of the N source concentration and the NH_4^+/NO_3^- ratio on phenylethanoid glycoside production was investigated for the first time in our study. NH_4^+ and NO_3^- are usually thought to modulate metabolism via enhancing growth and driving the TC towards more enhanced growth at the cost of production of less secondary metabolites. High carbon source to N source ratios in plant TCs usually lead to higher metabolite biosynthesis. As the growth speed decreases with the reduction of the relatively available N (or other limiting nutrient), the excess carbon pool is driven towards synthesis of secondary metabolites to a higher extent – thus, secondary metabolite accumulation often occurs after the period of maximum growth (Collin, 2001). In our case, however, none of the metabolite abundances were shown to be significantly influenced by GI itself (as shown by a linear model). If the N source would have been limiting in any of the media, GI would have likely been higher at higher N concentrations, but GI was unaffected by N concentration ($p = 0.54$). This suggests that the availability of NO_3^- and NH_4^+ in different ratios and net concentrations exerted more direct effects on biosynthesis of the examined NPs. These direct effects may include NH_4^+ acidity stress (George et al., 2007), or other, unknown pathways.

We can state, that while the widely used MSM is suboptimal with respect to NP abundance in the TCs, careful experimental design has to be implemented when reoptimizing the N source in the TC medium.

2.3.4. Simulated one-factor at a time optimization of natural product yields

As the abundance of several of the NPs were very good examples of the statistical interaction between the N source concentration and the NH_4^+/NO_3^- ratio, OFAT experiments were simulated in silico to assess the risk of ending up with a NP suboptimal yield. The inability to independently optimize media components was also suggested by Amdoun et al. (2009) (regarding NO_3^-/Ca^{2+}). Other studies also found, that NP accumulation depended on media N source, but the interactions between the NH_4^+/NO_3^- ratio and the N source concentrations could not be assessed for effects on the metabolome in most cases, because most studies used one-factor at a time strategy (Guo et al., 2005 and Wang and Tan, 2002), or did not use a factorial approach (Jacob and Malpathak, 2005).

To show the advantage of the FF strategy, four virtual optimization studies were carried out in silico. The interaction between the tested parameters and the consequence of using OFAT is perhaps best presented this way. The composition of the media was optimized in different OFAT regimes for each of the 89 NPs individually. The virtual experiments either started from MSM (60(0.33)) or 20(0). The optimization of the NH_4^+/NO_3^- ratio was followed by the optimization of the N source concentration or vice versa. In strategy #1, the starting medium was MSM and the virtual optimization began with the NH_4^+/NO_3^- ratio, followed by the virtual optimization of the N source concentration. In this scenario, 53 of the 89 NP abundances were suboptimal, with the suboptimal NPs showing a mean 1.56-fold abundance advantage in FF compared to the OFAT optima. The list of suboptimal media obtained by the different OFAT simulations for each NP is shown in Supplementary Table 2. Starting with medium 20(0) in strategy #2 resulted in similar results: 44 NP abundances were sub-optimal with the FF optima being 1.28-fold better on average. When the scheme was reversed to the experimental setup less common in the literature (N source concentration was optimized first in strategies #3–4), the OFAT performance substantially increased. Despite this, there were still 12 and 19 NPs sub-optimal abundance NPs, when starting from MSM or 20(0), respectively. The average fold advantage of the FF for these NPs was 1.30 and 1.37. For some NPs, the difference between the best FF and OFAT medium was greater, than 2-fold (Supplementary Table 2). It is also noteworthy, that the abundances of 6 NPs did not reach the FF optimum, regardless of the starting medium. Thus, if NP abundance optima are reached with OFAT, it can also simply be by chance. This chance can be increased however, by optimizing the N source concentration first, followed by the NH_4^+/NO_3^- ratio.

3. Conclusions

In this study, we successfully applied LC–ESI–MS^3 for the characterization of tissue cultures of a medicinal plant, P.*lanceolata* L. Many phenylethanoid glycosides previously not found in these calli were detected, and their structures were putatively identified.

The main goal of the study was to examine the effects of the N composition of the medium on the production of phenylethanoid glycosides and other NPs in *P. lanceolata* calli. Four N concentrations and four levels of the NH_4^+/NO_3^- ratio were tested in a full-factorial experiment enabling the estimation of interactions between these two parameters. Many conclusions could be drawn with regard to secondary metabolite production in medicinal plant tissue cultures.

The metabolomic approach was shown to be a powerful one when evaluating the results. The data processing and visualization procedures provided high throughput and highlighted most of the phenomena. The presented approach is therefore strongly encouraged when optimizing secondary metabolite production in in vitro cultures.

The original Murashige Skoog medium was found unsuitable for high yield production of phenylethanoid glycosides. In fact, it was one of the media with least NP abundances. The medium proposed by Budzianowska et al. (2004) for *P. lanceolata* tissue cultures was optimal for growth, but not NP production.

However, with the manipulation of the NH_4^+/NO_3^- ratio and N source concentration, very significant increase in the natural product accumulation could be achieved. Compared to the reference media, 1.5–3-fold increases in abundance were achieved for most metabolites. The highest NP abundance media were those with low N source concentrations (10 mM N). Thus, we have shown that a very simple and inexpensive modification of the medium can dramatically increase phenylethanoid glycoside yields. What is more, the manipulation of these parameters can also be easily implemented in industrial scale cultures, and is compatible with elicitations as well. The results suggest that N source composition must be re-optimized for optimal production of these natural products and that the two-stage culture strategy is to be preferred when tissue cultures are used for production of phenylethanoid glycosides.

For major metabolites, the maximum yields could be observed on different media: optimal plantamajoside production was achieved on 10(0.33), 3.54 ± 0.83% (dry wt.), while, in the case of acteoside, the best yield was 1.30 ± 0.40% (dry wt.) on 40(0.33). For most metabolites, the medium 10(0.33) was found to be optimal, for most of the others, 10(0) or 40(0.33).

Comparing the optimization strategies also led us to interesting conclusions. Interactions were detected between the two parameters for many metabolites – the response to the NH_4^+/NO_3^- ratio was not the same at different N source concentrations. The manipulation of the NH_4^+/NO_3^- ratio and N source concentrations has led to sub-optimal yields in case of in silico simulated one-factor at a time experimental designs, for many natural products. Therefore, factorial experiments with less repetitions must be preferred to one-factor at a time experiments with higher repetition counts. If OFAT is unavoidable due to some constraint, the N source concentration must be optimized first, as it was shown to lead to suboptimal yields much less often than OFAT protocols optimizing the NH_4^+/NO_3^- ratio first.

As the overall polyphenolic metabolite concentration was also heavily influenced by the tested parameters, our suggestions should be considered to be adopted when optimizing yields of other natural products in tissue cultures. These results are likely to apply for other metabolites, that are biosynthesized through the phenylpropanoid pathway.

4. Experimental

4.1. Chemicals

Purification of acteoside and plantamajoside was described previously, the structures were confirmed by NMR (Gonda et al., 2012 and Gonda et al., 2013). For all analytical applications, water purified with Arium 611 purification system (Sartorius) was used (conductivity 0.055 μS/cm). To obtain the LC/MS solvent mixtures, acetonitrile (Merck), formic acid (Baker), and the previously mentioned purified water was used. For the extractions, analytical reagent grade solvents methanol (VWR) and petrolether (40–60 °C, VWR) were used.

Components and additives of the Murashige–Skoog media (MSM) were of analytical grade, as listed below: boric acid (Reanal), calcium chloride (Reanal), cobalt(II)-chloride-hexahydrate (Reanal), copper-sulfate-pentahydrate (Reanal), disodium-EDTA (Reanal), iron(II)-sulfate (Reanal), magnesium-sulfate (Reanal), manganese sulfate (Reanal), sodium molybdenate (Reanal), potassium iodide

(Reanal), potassium nitrate (Reanal), potassium dihydrogen phosphate (Reanal), zinc sulfate heptahydrate (Reanal), myo-inozitol (Reanal), nicotinic acid (Reanal), ammonium nitrate (Reanal), sodium nitrate (Reanal), ammonium chloride (Reanal), potassium chloride (Reanal), pyridoxine hydrochloride (Carl Roth), thiamine hydrochloride (Carl Roth), saccharose (VWR), agar-agar (VWR), 2,4-dichlorophenoxyacetic acid (2,4-D) (Sigma Aldrich), benzyl-aminopurine (BAP) (Sigma Aldrich).

4.2. Tissue culture conditions and general protocols

All types of the modified MSM used contained 2% sucrose, Gamborg's vitamins, 0.8% agar–agar, the pH of the media was set to 5.8 prior to autoclaving. MSM refers to the original MSM composition (Murashige and Skoog, 1962), supplemented with the compounds listed above.

Calli were subcultured to the same medium composition every 28 days. Growth was calculated as growth index (GI) = (harvested mass − initial mass)/initial mass. To start a new culture, an accurately weighed initial mass of 100.0–150.0 mg of tissue was used. The callus lines were maintained under a photoperiod of 14/10 h (22/18 ± 2 °C in light/darkness). For illumination, white fluorescent light was used (10 μmol m−2 s−1).

4.3. Tissue culture initiation and line selection

Seeds of P.*lanceolata* were obtained from a local population near Hajdúsámson (Hungary) in 2008. The seeds were surface sterilized, and subcultured to MSM without NH_4NO_3, supplemented with 2% sucrose and 0.8% agar to germinate. After 7–10 days, the root tips were cut off, and subjected to MSM without $NH_4^+NO_3$, supplemented with 1 mg L^{-1} 2,4-D and 0.1 mg L^{-1} BAP for callus initiation (Budzianowska et al., 2004). Fifty lines were established. After a few months, ten stable, well-growing lines were screened for biosynthesis of PGs with TLC (Biringanine et al., 2006). A single clone – showing the presence of PGs in high concentrations – was selected for the N source study. It was deposited as "PL31" in our institute.

4.4. Effects of N source

To test the effects of the N source on the metabolite composition and content of P.*lanceolata* calli, Murashige–Skoog media (MSM) were prepared with different N source concentrations and NH_4^+/NO_3^- ratios.

The different concentrations of NH_4^+ and NO_3^- were obtained by adding stock solutions of NH_4NO_3, KNO_3, $NaNO_3$, NH_4Cl, KCl to the other ingredients of the 'basal' MSM (Murashige and Skoog, 1962). The final K+ concentration and the concentration of other major and minor ingredients was the same as in the original medium (Murashige and Skoog, 1962), except Cl^- and Na^+, which varied along the various media.

The NH_4^+/NO_3^- ratios tested were 1:2 (0.33), 1:4 (0.20), 1:8 (0.11), and 0:1 (0, NO_3^- only). The N source concentrations tested were 10, 20, 40 and 60 mM. The media are referred to as the codes 'N source concentration (NH_4^+/NO_3^- ratio)' throughout the manuscript. The original MSM is therefore referred to as '60(0.33)', and the medium used by Budzianowska et al. (2004), as '20(0)'. All combinations of the above were tested, yielding 16 types of media in total.

Segments of grown up calli from the maintenance medium 20(0) were subcultured to different media for the N source test. The experiment was performed in three repetitions. Each repetition was a set of two culture plates, that were pooled in the end of the 28 day incubation time.

4.5. LC–ESI–MS^3 instrument parameters

To obtain the best sensitivity during the experiments the instrument was tuned using acteoside (m/z 623 [M−H−]) in negative ion mode: a solution of acteoside (100 μg ml−1) in 20% MeCN + 0.1% formic acid in water was directly injected into the ion source by a syringe pump. The optimal ESI ionization parameters were as follows: heater temperature, 200 °C; sheath gas, N2; flow rate, 30 arbitrary units (arb); aux gas flow rate, 5 arb; spray voltage, 5 kV; capillary temperature, 275 °C; capillary voltage, −28,00 V. Sample quantification was run in negative ion mode (MS).

The LC–MS^n measurements were run on a Thermo Accela HPLC (column: Synergi C18 150 mm × 4.6 mm × 4 μm) attached to a Thermo LTQ XL Linear Ion Trap Mass Spectrometer. Gradient components were A, water with 0.1% formic acid; B, MeCN with 0.1% formic acid. The time program was 20% B: 0 → 2 min, 20 → 45% B: 2 → 20 min, 45 → 20% B: 20 → 21 min, 20% B 21 → 25 min. The HPLC gradient was adapted from Han et al. (2012). The injected sample amount was 1.0 μl in all cases.

4.6. Chemical analysis of *P. lanceolata* calli with LC–ESI–MS^3

For chemical analysis, harvested calli were dried in flowing warm air not exceeding 50 °C for 4 h, followed by removal of residual water by lyophilization. The dried calli were ground in mortars, and an accurately weighed sample (approximately 25 mg) was extracted with 1000 μl MeOH at 100 °C for 30 min. Then, 200 μl of the MeOH extracts was evaporated to dryness in vacuum, and extracted threefold with 1000 μl of petrolether (40–60 °C) to remove fat, and dried in vacuum again. Then, the defatted residues were reuptaken in 200 μl MeOH.

For the qualitative MS^3 characterization and identification of PGs in the samples, a 5-fold concentrated sample was injected (200 μl MeOH extract was dried and subsequently reuptaken in 40 μl MeOH, resulting in 125 mg dry wt. equivalent/ml). The chromatogram was evaluated with automatic fragmentation of the most intense MS1 peak or selected ions (CID energy 40%, activation time: 30 ms), followed by the automatic fragmentation of the most intense MS2 peak (same parameters).

For the quantification of major compounds (acteoside and plantamajoside), the reuptaken sample was diluted 100-fold with methanol (to 0.25 mg dry wt. equivalent/ml). Calibration curves from acteoside and plantamajoside were made in MeOH, concentration ranged from 1 to 20 μg ml−1. The method was found to be linear within this range (R2 > 0.99 for both analytes). For minor compounds, the sample was injected to the LC as is (25 mg dry wt. equivalent/ml). In these cases, only the MS1 total ion chromatograms were acquired. The minor compounds' abundance was in the useful linear range previously determined.

4.7. Identification of PGs

MS data were processed in Thermo Excalibur version 2.2 SP1.48, and MZmine 2.10 freeware (Pluskal et al., 2010). $[M-H]^-$ → MS2 → MS^3 peak lists were created according to the guides to MZMine. Chief fragmentation patterns of PGs were evaluated on basis of Han et al., 2012, Li et al., 2009, Petreska et al., 2011 and Qi et al., 2012 and Shi et al. (2013). Frequently found fragments and neutral loss values were interpreted by literature review and comparison with chief fragmentation routes of our standards (acteoside and plantamajoside).

4.8. Effects of N source on the pattern and concentration of natural products in *P. lanceolata* calli

Peaks in selected extracted ion chromatograms were integrated in all samples with Thermo Excalibur software, using settings optimized for integration of each m/z, resulting in 186 peaks. This peak list contained all major peaks in the TIC. Only $[M-H]^-$ ions present in at least 75% of the samples and of a median nominal abundance above 750 were considered for further quantitative analysis. This filtered dataset was filtered again to remove typical negative ion mode adducts (e.g. M+HCOOH-H, M+AcOH-H) and isotopes (M+1-H). Finally, a dataset containing the abundance data of 89 metabolites was subjected to a data-mining workflow to evaluate the effects of the N source composition on the abundance of individual metabolites.

The scaled and centered dataset was submitted to hierarchical clustering analysis using Manhattan distance and Ward's method. The bootstrapped resampling of the cluster tree was implemented in R, using pvclust 1.2–2, n = 25000 (Suzuki and Shimodaira, 2006). The correlation matrix for the NPs found was also obtained, and examined as a correlation heatmap. The effects of different treatments on the selected NPs were also examined, using heatmap plots of the unscaled raw abundance data, presenting interactions between N source concentration and NH_4^+/NO_3^- ratio. For these plots, linear interpolation was carried out between measured data points. Figure generating scripts were implemented in R, using ggplot 0.9.3.1 (Wickham, 2009).

To obtain information on the effects of the N source concentration and the NH_4^+/NO_3^- ratio on the metabolome as a whole, scaled and centered abundance data (3 replicates for each medium) were subjected to principal component analysis in R. Scaling and centering (the NP abundances were brought to zero mean and variance of one) was accomplished so that all NPs have the same weight in the analysis.

4.9. Statistical analyses

The effects of NH_4^+/NO_3^- ratio and the N source concentration on the metabolite abundances were checked for significant differences using multi-way ANOVAs. ANOVA was preferred to linear models throughout the work, because the relationships between the two treatments and the responses were non-linear. So, the N source concentrations and NH_4^+/NO_3^- ratio are subjected to analysis as categorical variables, with the response (abundances of NPs) being a continuous variable. As a high number of hypotheses are usually tested in metabolomic studies, additional measures have to be taken in order to avoid false positive hypothesis tests (Broadhurst and Kell, 2006). For its simplicity and easy implementation, Bonferroni correction was chosen to be applied to the resulting p values of the significance tests. Therefore, p values were only considered significant, if they were below $p < 0.05/n$, where n is the number of tested hypotheses in the study (Broadhurst and Kell, 2006), thus the significance levels * $p < 0.00011$; ** $p < 2.25e\text{-}4$; *** $p < 2.25e\text{-}5$ were used. Statistical evaluations were implemented in R 3.0.1 (R Development Core Team, 2009).

4.10. Simulated one-factor at a time experiments

We computationally simulated one-factor at a time (OFAT) experiments with the full-factorial results in hand. Four types of in silico simulations were done. In all types, the optimization of the first factor is followed by the other. In the second part, the first factor is kept at the previously found optimum. The computation is done for each NP abundance separately. In strategy #1, the starting medium was MSM 60(0.33), NH_4^+/NO_3^- ratio was optimized first (testing of 60(0), 60(0.11), 60(0.20) and 60(0.33)). Then, after selecting the medium with highest NP abundance, the N source concentration was subject to optimization. The best medium of the OFAT virtual optimization study was then compared to the best medium of the full-factorial study. In strategy #3, the starting medium was the same, but N source

concentration was optimized first (testing of 10(0.33), 20(0.33), 40(0.33) and 60(0.33)). After selecting the medium with highest NP abundance, the NH_4^+/NO_3^- ratio was optimized. Strategies #2 and #4 were analogous to #1 and #3, respectively, but the starting medium was medium 20(0), proposed by Budzianowska et al. (2004) for *P. lanceolata* tissue culture.

Acknowledgments
The authors declare, that they share no conflict of interest. The research was supported by the EU and co-financed by the European Social Fund under the project ENVIKUT (TÁMOP-4.2.2.A-11/1/KONV-2012-0043), and OTKA K 81370 and OTKA PD 112374 research grants. This research was also supported by the European Union and the State of Hungary, co-financed by the European Social Fund in the framework of TÁMOP 4.2.4. A/2-11-1-2012-0001 'National Excellence Program'. The work was supported by the BAROSS REG_EA_09-1-2009-0028 (LCMS_TAN) grant as well as the TÁMOP 4.2.1./B-09/1/KONV-2010-0007 project. The project is implemented through the New Hungary Development Plan, co-financed by the European Social Fund and the European Regional Development Fund.

References

Amdoun, R., Khelifi, L., Khelifi-Slaoui, M., Amroune, S., Benyoussef, E.-H., Thi, D.V., Assaf-Ducrocq, C., Gontier, E., 2009. Influence of minerals and elicitation on Datura stramonium L. tropane alkaloid production: modelization of the in vitro biochemical response. Plant Sci. 177, 81–87.

Beara, I., Lesjak, M., Jovin, E., Balog, K., Anackov, G., Orcic, D., Mimica-Dukic, N., 2009. Plantain (*Plantago* L.) species as novel sources of flavonoid antioxidants. J. Agric. Food Chem. 57, 9268–9273. http://dx.doi.org/10.1021/jf902205m.

Biringanine, G., Chiarelli, M., Faes, M., Duez, P., 2006. A validation protocol for the HPTLC standardization of herbal products: application to the determination of acteoside in leaves of *Plantago* palmata Hook. f.s. Talanta 69, 418–424. http://dx.doi.org/10.1016/j.talanta.2005.10.007.

Broadhurst, D.I., Kell, D.B., 2006. Statistical strategies for avoiding false discoveries in metabolomics and related experiments. Metabolomics 2, 171–196. http://dx.doi.org/10.1007/s11306-006-0037-z.

Budzianowska, A., Skrzypczak, L., Budzianowski, J., 2004. Phenylethanoid glucosides from in vitro propagated plants and callus cultures of *Plantago lanceolata*. Planta Med. 70, 834–840. http://dx.doi.org/10.1055/s-2004-827232.

Collin, H., 2001. Secondary product formation in plant tissue cultures. Plant Growth Regul. 34, 119–134.

Fons, F., Gargadennec, A., Rapior, S., 2008. Culture of *Plantago* species as bioactive components resources: a 20-year review and recent applications. Acta Bot. Gallica 155, 277–300.

Fons, F., Tousch, D., Rapior, S., Gueiffier, A., Roussel, J., Gargadennec, A., Andary, C., 1999. Phenolic profiles of untransformed and hairy root cultures of *Plantago lanceolata*. Plant Physiol. Biochem. 37, 291–296.

Fu, G., Pang, H., Wong, Y.H., 2008. Naturally occurring phenylethanoid glycosides: potential leads for new therapeutics. Curr. Med. Chem. 15, 2592–2613.

George, E.F., Hall, M.A., Klerk, G.-J.D., 2007. Plant Propagation by Tissue Culture: Volume 1. The Background, first ed. Springer, pp. 71, 73, 186.

Gonda, S., Kiss, A., Emri, T., Batta, G., Vasas, G., 2013. Filamentous fungi from *Plantago lanceolata* L. leaves: contribution to the pattern and stability of bioactive metabolites. Phytochemistry 86, 127–136. http://dx.doi.org/10.1016/j.phytochem.2012.10.017.

Gonda, S., Toth, L., Gyemant, G., Braun, M., Emri, T., Vasas, G., 2012. Effect of high relative humidity on dried *Plantago lanceolata* L. leaves during long-term storage: effects on chemical

composition, colour and microbiological quality. Phytochem. Anal. 23, 88–93. http://dx.doi.org/10.1002/pca.1329.

Guarnerio, C.F., Fraccaroli, M., Gonzo, I., Pressi, G., Toso, R.D., Guzzo, F., Levi, M., 2012. Metabolomic analysis reveals that the accumulation of specific secondary metabolites in Echinacea angustifolia cells cultured in vitro can be controlled by light. Plant Cell Rep. 31, 361–367. http://dx.doi.org/10.1007/s00299-011-1171-2.

Guo, X., Gao, W., Xiao, P., 2005. Factors affecting root growth and metabolite production in Salvia miltiorrhiza adventitious root cultures. Minerva Biotechnol. 17, 133–139.

Han, L., Boakye-Yiadom, M., Liu, E., Zhang, Y., Li, W., Song, X., Fu, F., Gao, X., 2012. Structural characterisation and identification of phenylethanoid glycosides from Cistanches deserticola Y.C. Ma by UHPLC/ESI-QTOF-MS/MS. Phytochem. Anal. PCA 23, 668–676. http://dx.doi.org/10.1002/pca.2371.

Harvey, A.L., 2008. Natural products in drug discovery. Drug Discov. Today 13, 894–901.

Hirasuna, T., Shuler, M., Lackney, V., Spanswick, R., 1991. Enhanced anthocyanin production in grape cell-cultures. Plant Sci. 78, 107–120. http://dx.doi.org/10.1016/0168-9452(91)90167-7.

Jacob, A., Malpathak, N., 2005. Manipulation of MS and B5 components for enhancement of growth and solasodine production in hairy root cultures of Solanum khasianum Clarke. Plant Cell, Tissue Organ Cult. 80, 247–257. http://dx.doi.org/10.1007/s11240-004-0740-2.

Jin, Q., Jin, H.-G., Shin, J.-E., Hong, J.-K., Woo, E.-R., 2011. Phenylethanoid glycosides from Digitalis purpurea L. Bull. Korean Chem. Soc. 32, 1721–1724. http://dx.doi.org/10.5012/bkcs.2011.32.5.1721.

Kırmızıbekmez, H., Montoro, P., Piacente, S., Pizza, C., Dönmez, A., Calıs, I., 2005. Identification by HPLC-PAD-MS and quantification by HPLC-PAD of phenylethanoid glycosides of five Phlomis species. Phytochem. Anal. 16, 1–6.

Li, L., Liu, C., Liu, Z., Tsao, R., Liu, S., 2009. Identification of phenylethanoid glycosides in plant extract of *Plantago* asiatica L. by liquid chromatography–electrospray ionization mass spectrometry. Chin. J. Chem. 27, 541–545. http://dx.doi.org/10.1002/cjoc.200990088.

Mederos, S., Martin, C., Navarro, E., Ayuso, M.J., 1997. Micropropagation of a medicinal plant, *Plantago* major L. Biol. Plant. 40, 465–468. http://dx.doi.org/10.1023/A:1001190603295.

Murashige, T., Skoog, F., 1962. A revised medium for rapid growth and bioassays with tobacco tissue cultures. Physiol. Plant. 15, 473–497.

Gonda, S., Toth, L., Gyemant, G., Braun, M., Emri, T., Vasas, G., 2012. Effect of high relative humidity on dried *Plantago lanceolata* L. leaves during long-term storage: effects on chemical composition, colour and microbiological quality. Phytochem. Anal. 23, 88–93. http://dx.doi.org/10.1002/pca.1329.

Guarnerio, C.F., Fraccaroli, M., Gonzo, I., Pressi, G., Toso, R.D., Guzzo, F., Levi, M., 2012. Metabolomic analysis reveals that the accumulation of specific secondary metabolites in Echinacea angustifolia cells cultured in vitro can be controlled by light. Plant Cell Rep. 31, 361–367. http://dx.doi.org/10.1007/s00299-011-1171-2.

Guo, X., Gao, W., Xiao, P., 2005. Factors affecting root growth and metabolite production in Salvia miltiorrhiza adventitious root cultures. Minerva Biotechnol. 17, 133–139.

Han, L., Boakye-Yiadom, M., Liu, E., Zhang, Y., Li, W., Song, X., Fu, F., Gao, X., 2012. Structural characterisation and identification of phenylethanoid glycosides from Cistanches deserticola Y.C. Ma by UHPLC/ESI-QTOF-MS/MS. Phytochem. Anal. PCA 23, 668–676. http://dx.doi.org/10.1002/pca.2371.

Harvey, A.L., 2008. Natural products in drug discovery. Drug Discov. Today 13, 894–901.

Hirasuna, T., Shuler, M., Lackney, V., Spanswick, R., 1991. Enhanced anthocyanin production in grape cell-cultures. Plant Sci. 78, 107–120. http://dx.doi.org/10.1016/0168-9452(91)90167-7.

Jacob, A., Malpathak, N., 2005. Manipulation of MS and B5 components for enhancement of growth and solasodine production in hairy root cultures of Solanum khasianum Clarke. Plant Cell, Tissue Organ Cult. 80, 247–257. http://dx.doi.org/10.1007/s11240-004-0740-2.

Jin, Q., Jin, H.-G., Shin, J.-E., Hong, J.-K., Woo, E.-R., 2011. Phenylethanoid glycosides from Digitalis purpurea L. Bull. Korean Chem. Soc. 32, 1721–1724. http://dx.doi.org/10.5012/bkcs.2011.32.5.1721.

Kırmızıbekmez, H., Montoro, P., Piacente, S., Pizza, C., Dönmez, A., Calıs, I., 2005. Identification by HPLC-PAD-MS and quantification by HPLC-PAD of phenylethanoid glycosides of five Phlomis species. Phytochem. Anal. 16, 1–6.

Li, L., Liu, C., Liu, Z., Tsao, R., Liu, S., 2009. Identification of phenylethanoid glycosides in plant extract of *Plantago* asiatica L. by liquid chromatography–electrospray ionization mass spectrometry. Chin. J. Chem. 27, 541–545. http://dx.doi.org/10.1002/cjoc.200990088.

Mederos, S., Martin, C., Navarro, E., Ayuso, M.J., 1997. Micropropagation of a medicinal plant, *Plantago* major L. Biol. Plant. 40, 465–468. http://dx.doi.org/10.1023/A:1001190603295.

Murashige, T., Skoog, F., 1962. A revised medium for rapid growth and bioassays with tobacco tissue cultures. Physiol. Plant. 15, 473–497.

Petreska, J., Stefkov, G., Kulevanova, S., Alipieva, K., Bankova, V., Stefova, M., 2011. Phenolic compounds of mountain tea from the Balkans: LC/DAD/ESI/MSn profile and content. Nat. Prod. Commun. 6, 21–30.

Pluskal, T., Castillo, S., Villar-Briones, A., Orešič, M., 2010. MZmine 2: modular framework for processing, visualizing, and analyzing mass spectrometry-based molecular profile data. BMC Bioinformatics 11, 395. http://dx.doi.org/10.1186/1471-2105-11-395.

Qi, M., Xiong, A., Geng, F., Yang, L., Wang, Z., 2012. A novel strategy for target profiling analysis of bioactive phenylethanoid glycosides in *Plantago* medicinal plants using ultra-performance liquid chromatography coupled with tandem quadrupole mass spectrometry. J. Sep. Sci. 35, 1470–1478. http://dx.doi.org/10.1002/jssc.201200010.

R Development Core Team, 2009. R: A Language and Environment for Statistical Computing. Austria, Vienna.

Ronsted, N., Franzyk, H., Molgaard, P., Jaroszewski, J., Jensen, S., 2003. Chemotaxonomy and evolution of *Plantago* L. Plant Syst. Evol. 242, 63–82. http://dx.doi.org/10.1007/s00606-003-0057-3.

Schmidt, S., Jakab, M., Jav, S., Streif, D., Pitschmann, A., Zehl, M., Purevsuren, S., Glasl, S., Ritter, M., 2013. Extracts from Leonurus sibiricus L. increase insulin secretion and proliferation of rat INS-1E insulinoma cells. J. Ethnopharmacol. 150, 85–94.

Shi, Y., Wu, C., Chen, Y., Liu, W., Feng, F., Xie, N., 2013. Comparative analysis of three Callicarpa herbs using high performance liquid chromatography with diode array detector and electrospray ionization–trap mass spectrometry method. J. Pharm. Biomed. Anal. 75, 239–247. http://dx.doi.org/10.1016/j.jpba.2012.11.038.

Suzuki, R., Shimodaira, H., 2006. Pvclust: an R package for assessing the uncertainty in hierarchical clustering. Bioinformatics 22, 1540–1542. http://dx.doi.org/10.1093/bioinformatics/btl117.

Wang, J., Tan, R., 2002. Artemisinin production in Artemisia annua hairy root cultures with improved growth by altering the nitrogen source in the medium. Biotechnol. Lett. 24, 1153–1156.

Wickham, H., 2009. ggplot2: Elegant Graphics for Data Analysis, 2nd Printing. ed. Springer.

Wu, C.-H., Dewir, Y.H., Hahn, E.-J., Paek, K.-Y., 2006. Optimization of culturing conditions for the production of biomass and phenolics from adventitious roots of Echinacea angustifolia. J. Plant Biol. 49, 193–199. http://dx.doi.org/10.1007/BF03030532.

Zhao, J., Davis, L.C., Verpoorte, R., 2005. Elicitor signal transduction leading to production of plant secondary metabolites. Biotechnol. Adv. 23, 283–333. http://dx.doi.org/10.1016/j.biotechadv.2005.01.003.

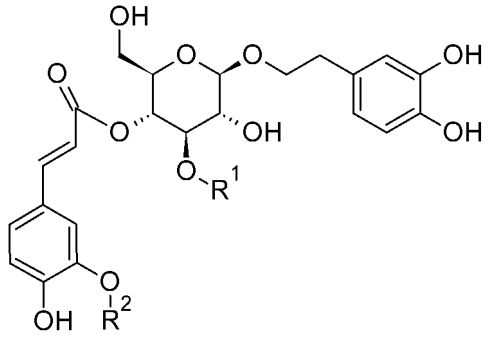

Fig. 1. Selected phenylethanoid glycosides detected from the MeOH extracts of *P. lanceolata* calli by LC–ESI–MS^3. Plantamajoside, R1 = Glc, R2 = H; Acteoside, R1 = Rha, R2 = H; Desrhamnosyl-acteoside, R1 = R2 = H; Lavandulifolioside, R1 = Ara(1->2)Rha, R2 = H; Leucosceptoside A, R1 = Rha, R2 = Me. For details of identification, see text and Table 1. Abbreviations: Ara, arabinose; Glc, glucose; Rha, rhamnose.

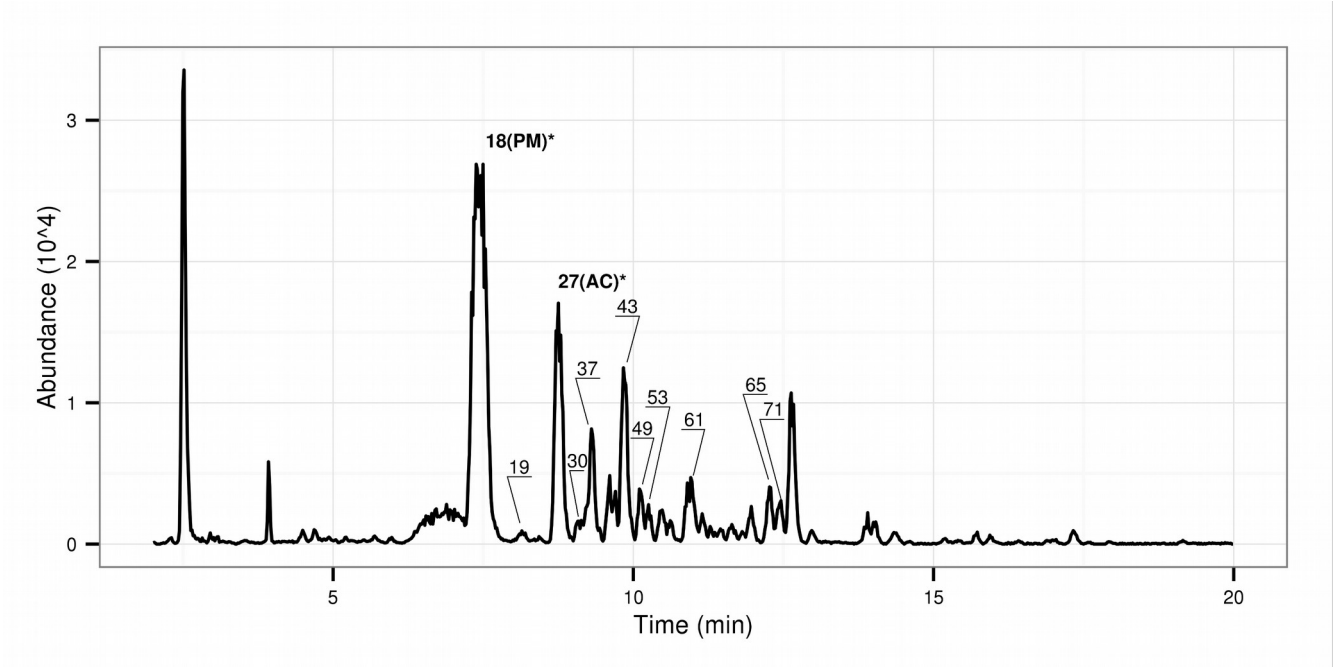

Fig. 2. LC–ESI–MS chromatogram of the MeOH extract of a *P. lanceolata* callus grown on medium 10(0.33) (25 mg dry wt./ml, total ion chromatogram in negative ion mode). Note that in this injection, the area under curve of plantamajoside was beyond the linear range of determination, and thus, major NPs were quantified in the 100-fold dilution, and not from the chromatogram presented here. Main peaks are marked with the metabolite numbers used in text, see Table 1 for putative identification. NPs compared with standards are marked with an asterisk. For m/z values, and putative identification, see Table 1. Abbreviations: AC, acteoside; PM, plantamajoside.

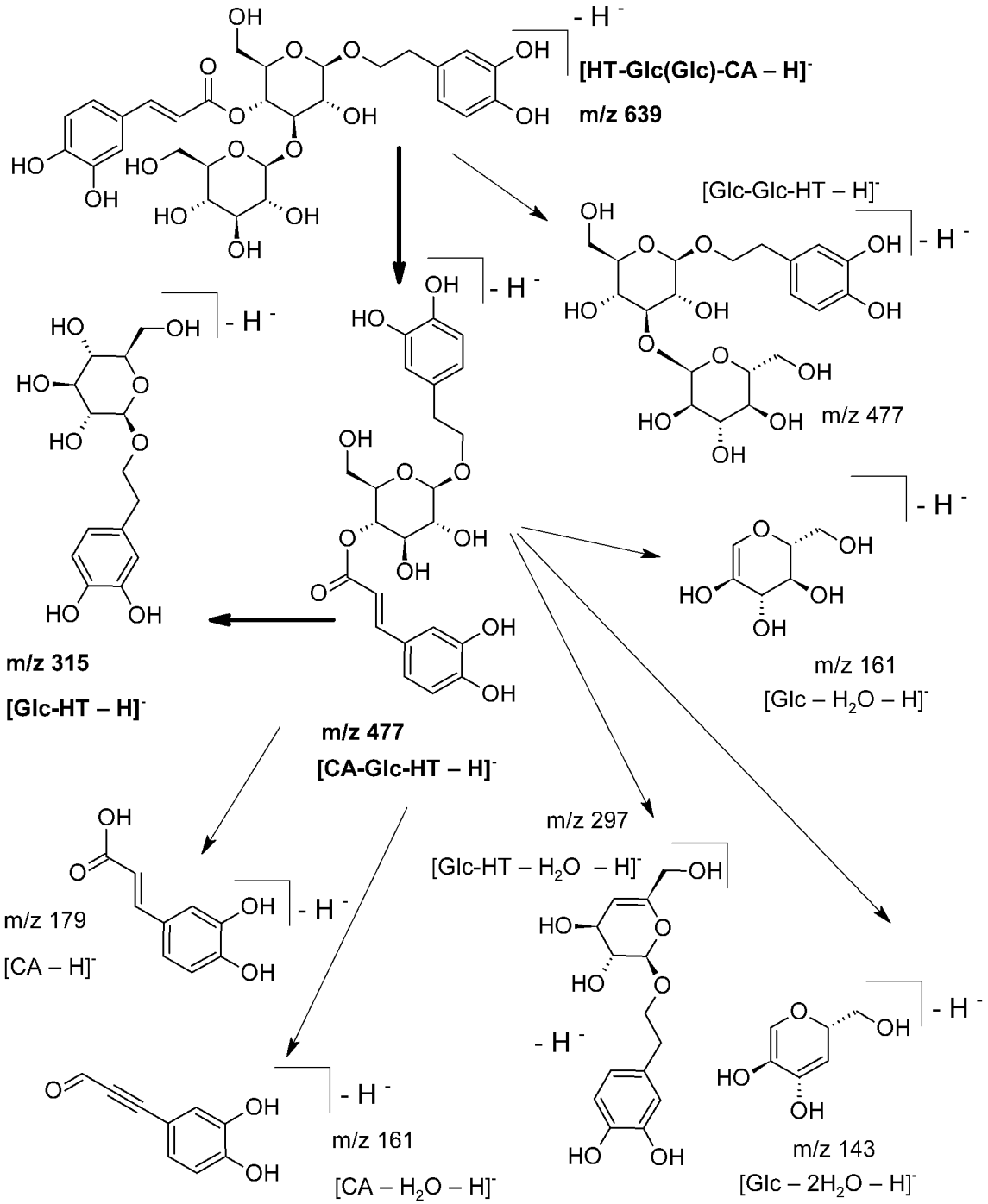

Fig. 3. Proposed fragmentation pattern of plantamajoside, the main phenylethanoid glycoside of the *P. lanceolata* callus extract in negative mode LC–ESI–MS^3. The main fragmentation route is highlighted with bold arrows and bold font.

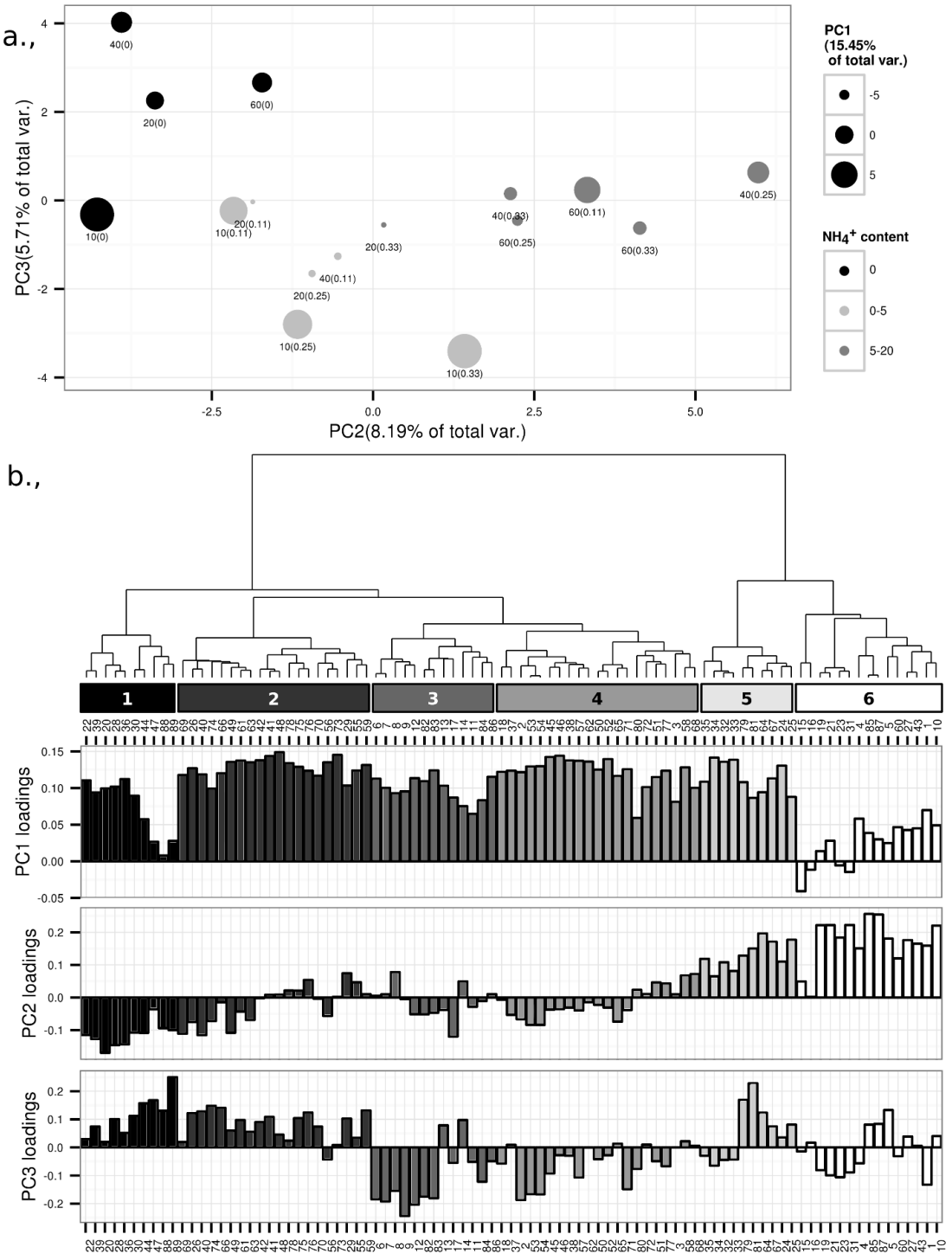

Fig. 4. Principal component (PC) analysis score plot of the scaled, centered and per-composition averaged natural product abundance dataset. The plot shows the effect of media composition on the metabolome as a whole. The NP abundances were measured by LC–ESI–MS^3 from MeOH extracts of *P. lanceolata* calli grown on media with different N source compositions. For more details, see text. Subplots: (a) Pseudo-3D score plot of PCs 1–3. PC2 and PC3 scores are plotted on axes x and y, respectively, while PC1 is made proportional to point size (see legend). Media codes are as follows: N concentration (mM), followed by NH_4^+/NO_3^- ratio (ratio of NH_4^+ in the total N source) in parentheses.

The NH_4^+ concentration in the media is coded by color (see legend). Abbreviations: NSC, N source concentration. (b), Loading plot for the first three PCs showing contribution of the 89 individual metabolites to the PC scores. The order of NPs was obtained from hierarchical cluster analysis of the NP abundances.

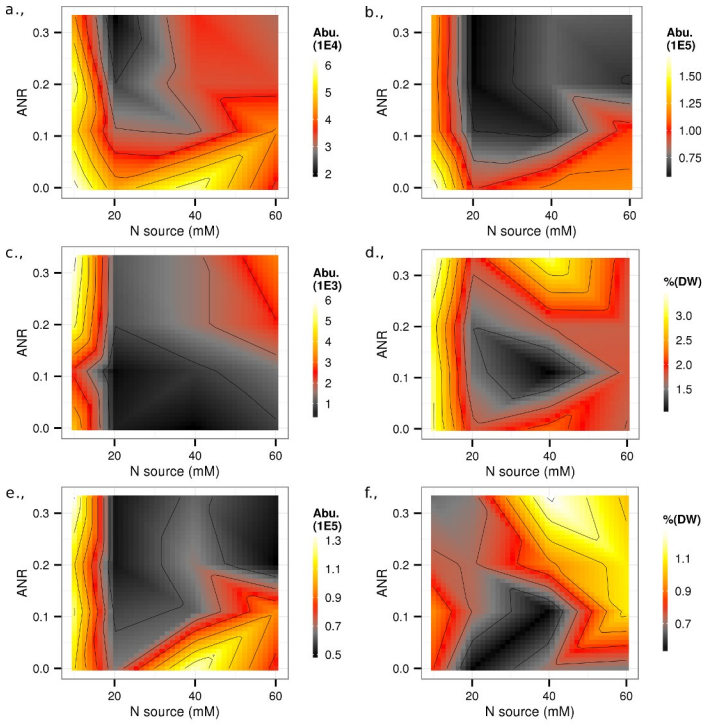

Fig. 5. Abundance of selected natural products from extracts of *P. lanceolata* calli grown on media with different N source concentrations and NH_4^+/NO_3^- ratios (ratio of $NH_4^+$the total N source). Color is proportional to the abundance (area under curve) for the given NPs, quantified in extracted ion chromatograms (a, b, c, e), or content of dry weight expressed as percent (d, f) Subplots: (a), **22**, putatively identified as desrhamnosyl-acteoside, cluster 1; (b), **49**, a plantamajoside isomer, cluster 2; (c), **8**, putatively identified as a plantamajoside hexoside, cluster 3; (d), **18**, plantamajoside (plantamajoside), cluster 4; (e), **65**, putatively identified as a dimethyl-acetyl acteoside, cluster 4; (f), **27**, acteoside, cluster 6.

Table 1.
Fragmentation pattern of putatively identified major peaks obtained by LC–ESI–MS^3 analysis of defatted Plantago lanceolata calli MeOH extracts in negative ion mode. MS2 ions are CID products of the $[M-H]^-$, while MS^3 ions are CID products of the most abundant MS^2 ion ($MS^{2\,a}$).

Abbreviations: Ara, arabinose; CA, caffeic acid; Glc, glucose; HT, hydroxytyrosol; MeCA, methyl caffeic acid; Me2CA, dimethyl caffeic acid; MeHT, methyl-hydroxytyrosol; Rha, rhamnose, Rt, retention time (minutes). Metabolites that were identical with standards, are marked with an asterisk. For identification and references, see text.

[a] Most intensive MS^2 ion, subjected to CID, with daughter ions shown in column 'MS^3'.

[b] MS^2 ions not fragmented further.

#	Rt	Putative identification	Structure of $[M-H]^-$	$[M-H]^-$	$MS^{2\,b}$	$MS^{2\,b}$	MS^3
8	4.85	Plantamajoside hexoside	[HT-Glc(Glc)(Glc)-CA – H]$^-$	801	639		477
18	8.08	Plantamajoside *	[HT-Glc(Glc)-CA – H]$^-$	639	477	315	135, 143, 161, 179, 297, 315
19	8.16	Lavandulifolioside	[HT-Glc(Rha(Ara))-CA – H]$^-$	755	593	443, 447, 461, 575, 609, 623	461, 447
22	9.07	Desrhamnosylacteoside	[HT-Glc-CA – H]$^-$	477	161	135, 179, 203, 315, 323, 341	133
27	9.31	Acteoside *	[HT-Glc(Rha)-CA – H]$^-$	623	461	315, 443, 477	135, 161, 297, 315
30	9.61	Desrhamnosylacteoside 2	[HT-Glc-CA – H]$^-$	477	161	179, 251, 281, 315	133
37	9.88	Plantamajoside 2	[HT-Glc(Glc)-CA – H]$^-$	639	477	315	135, 143, 161, 179, 297, 315
43	10.45	Acteoside 2	[HT-Glc(Rha)-CA – H]$^-$	623	461	315, 443, 477	135, 161, 297, 315
49	10.54	Plantamajoside 3	[HT-Glc(Glc)-CA – H]$^-$	639	477	251, 315	161, 315
53	11.00	Methyl-plantamajoside	[HT-Glc(Glc)-MeCA – H]$^-$	653	607	491	315, 443, 461
59	11.63	Methyl acteoside (leucosceptoside A)	[HT-Glc(Rha)-MeCA – H]$^-$	637	461	443, 475, 491	135, 315
61	11.84	Methyl-plantamajoside 2	[HT-Glc(Glc)-MeCA – H]$^-$	653	477	459, 491	315
64	11.97	Dimethyl-plantamajoside	[MeHT-Glc(Glc)-MeCA – H]$^-$	667	473	193, 491, 505	311
65	12.30	Dimethyl-acetyl-acteoside	[HT-Glc(Ac)(Rha)-Me2CA – H]$^-$	693	649		443, 461, 485, 503, 589, 607
71	12.64	Dimethyl-acetyl-	[HT-Glc(Ac)(Rha)-	693	649		443, 461, 485,

		acteoside 2	Me2CA – H]$^-$				503, 589, 607

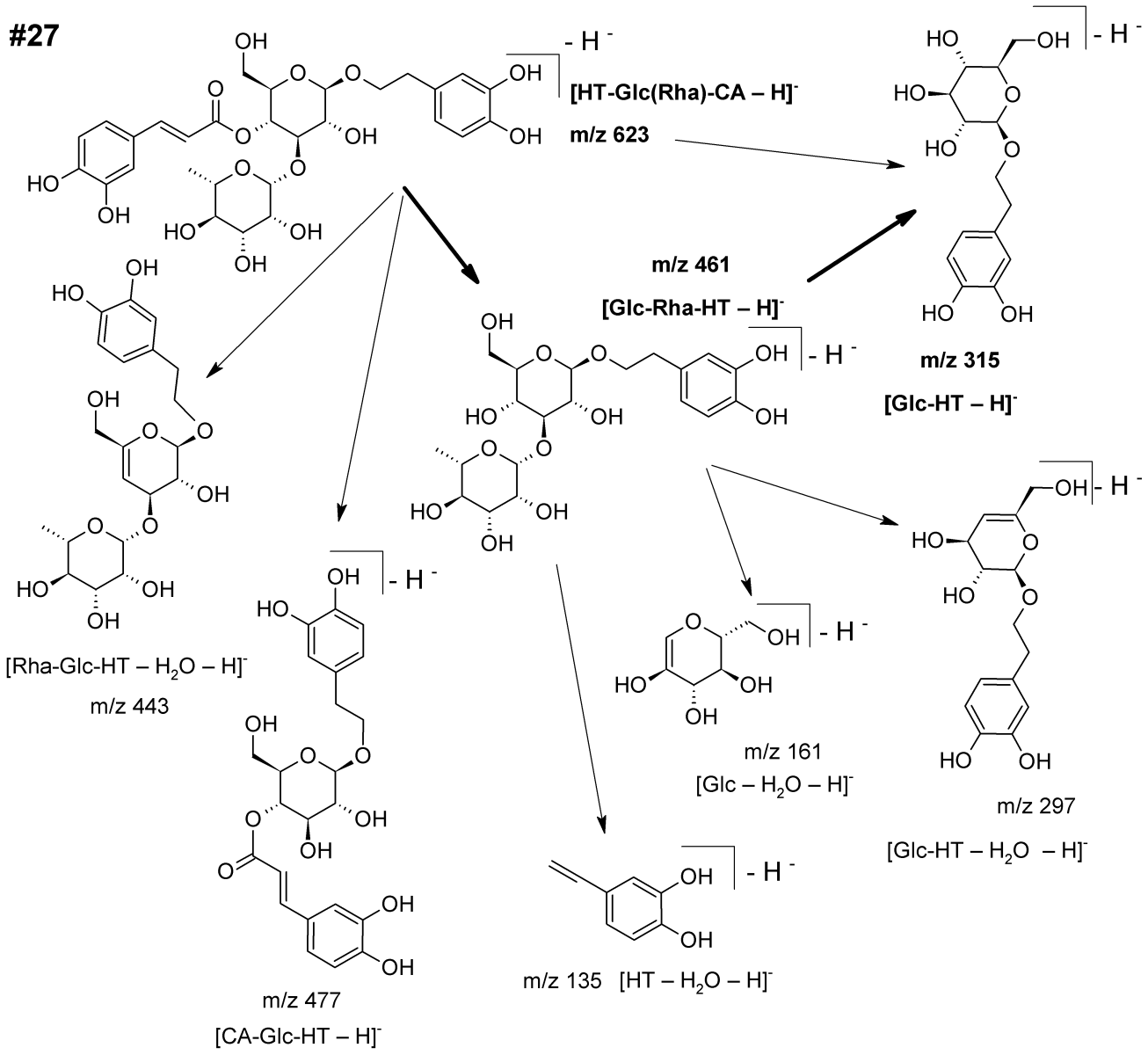

Supplementary Figure 1. Proposed fragmentation pattern of acteoside (**#27**), one of the main phenylethanoid glycosides of the *P. lanceolata* callus extract in negative mode LC-ESI-MS^3. The main fragmentation route is highlighted with bold arrows and bold font.

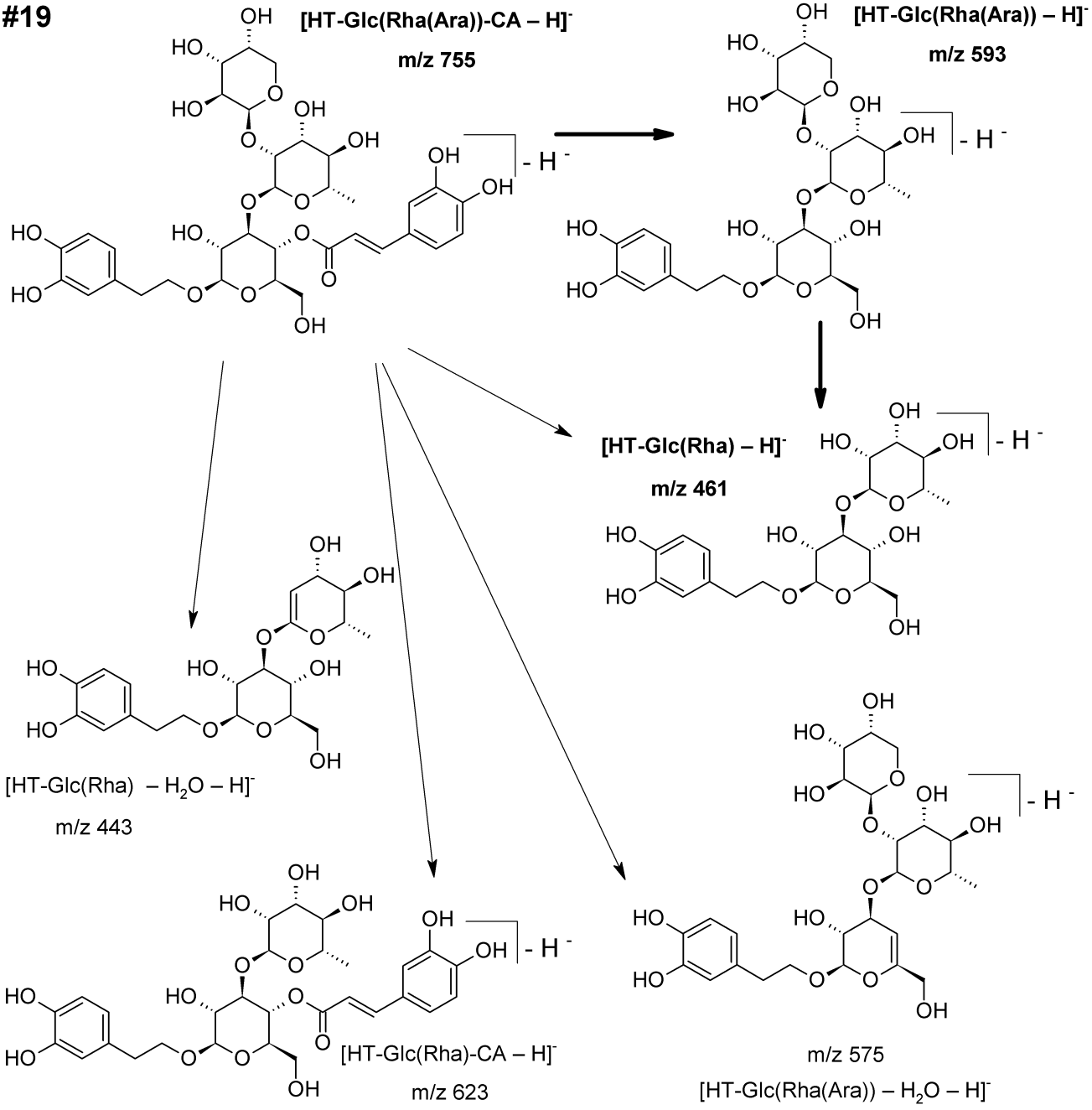

Supplementary Figure 2. Proposed fragmentation pattern of **#19**, identified as lavandulifolioside. This natural product is one of the phenylethanoid glycosides of the *P. lanceolata* callus extract detected by negative mode LC-ESI-MS^3. The main fragmentation route is highlighted with bold arrows and bold font.

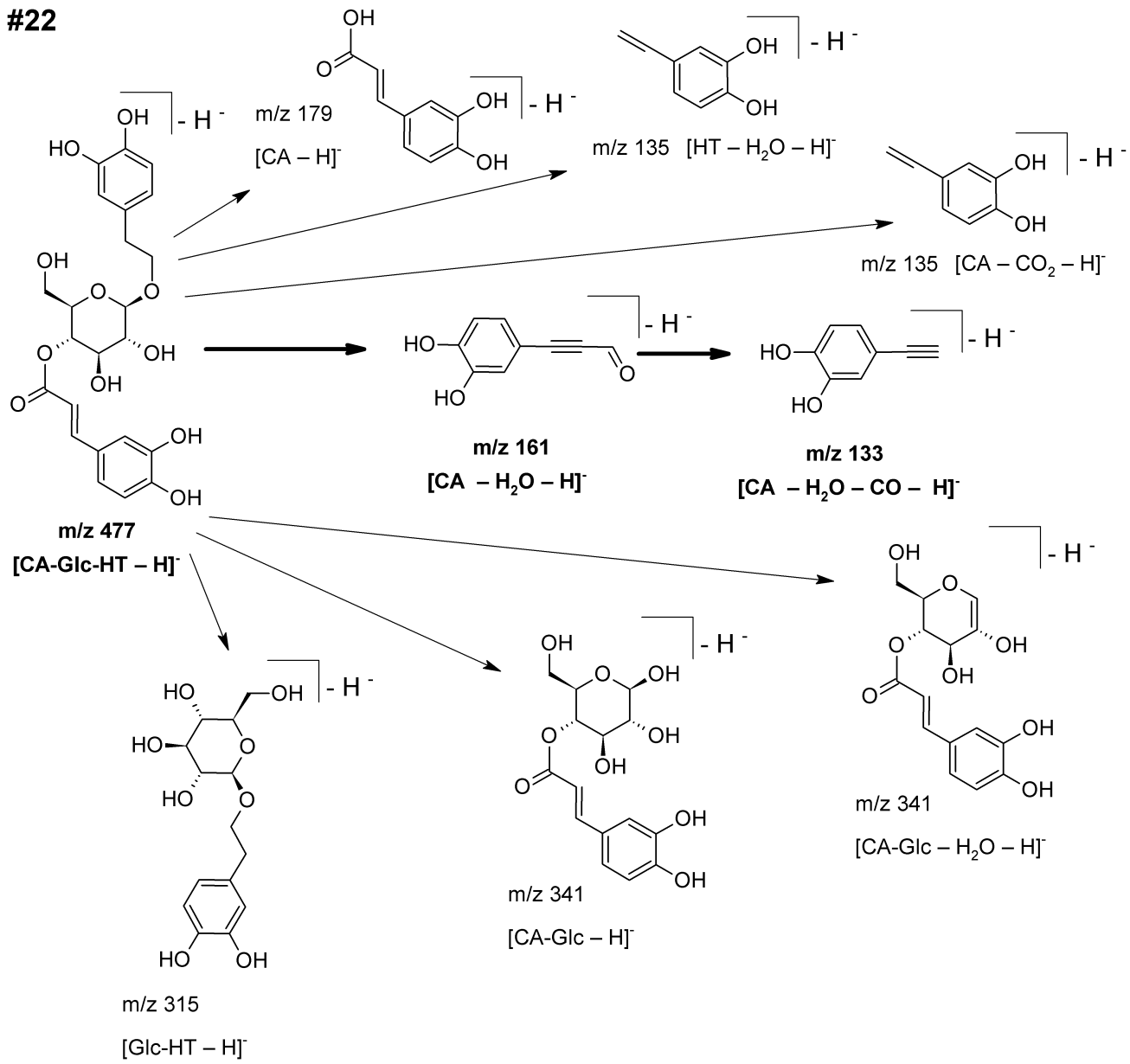

Supplementary Figure 3. Proposed fragmentation pattern of **#22**, identified as desrhamnosylacteoside (=Calceorioside B). This natural product is one of the phenylethanoid glycosides of the *P. lanceolata* callus extract detected by negative mode LC-ESI-MS^3. The main fragmentation route is highlighted with bold arrows and bold font.

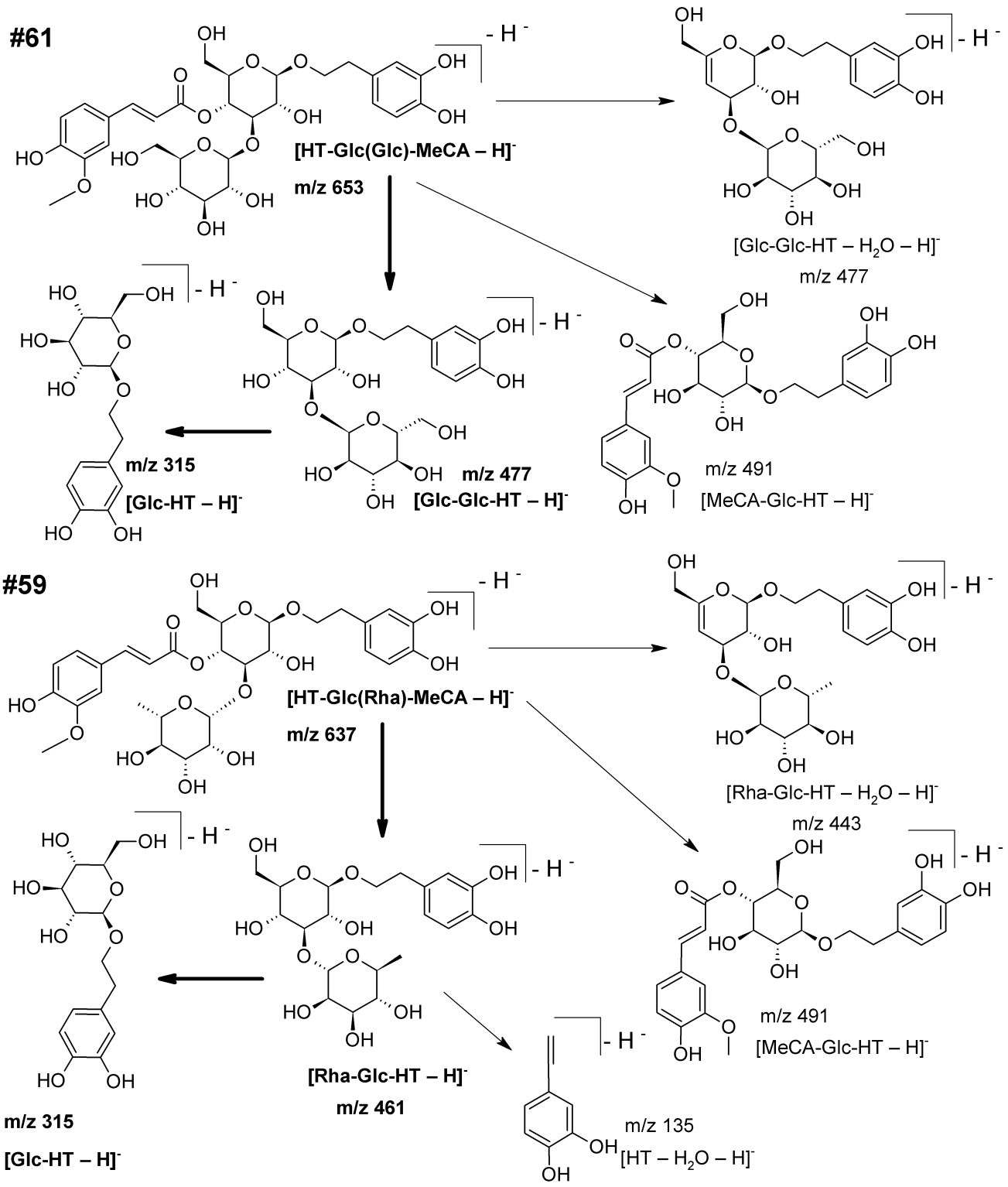

Supplementary Figure 4. Proposed fragmentation pattern of **#61** and **#59** identified as methyl-plantamajoside and leucosceptoside A (methyl-acteoside), respectively. Note similar patterns of fragmentation. These natural products are phenylethanoid glycosides of the *P. lanceolata* callus extract detected by negative mode LC-ESI-MS^3. The main fragmentation route is highlighted with bold arrows and bold font.

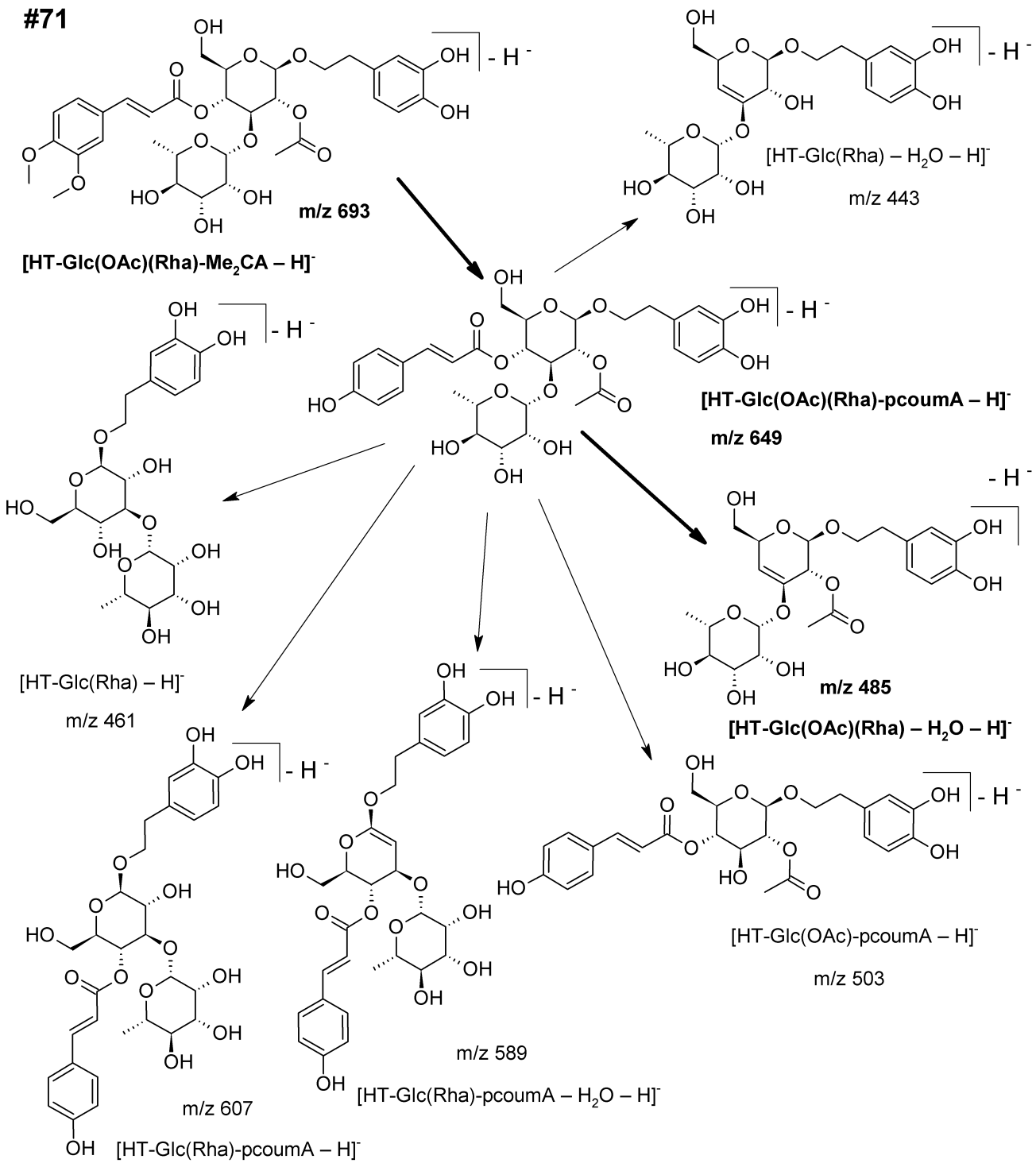

Supplementary Figure 5. Proposed fragmentation pattern of **#71**, identified as dimethyl-acetyl-acteoside. This natural product is one of the phenylethanoid glycosides of the *P. lanceolata* callus extract detected by negative mode LC-ESI-MS^3. The main fragmentation route is highlighted with bold arrows and bold font.

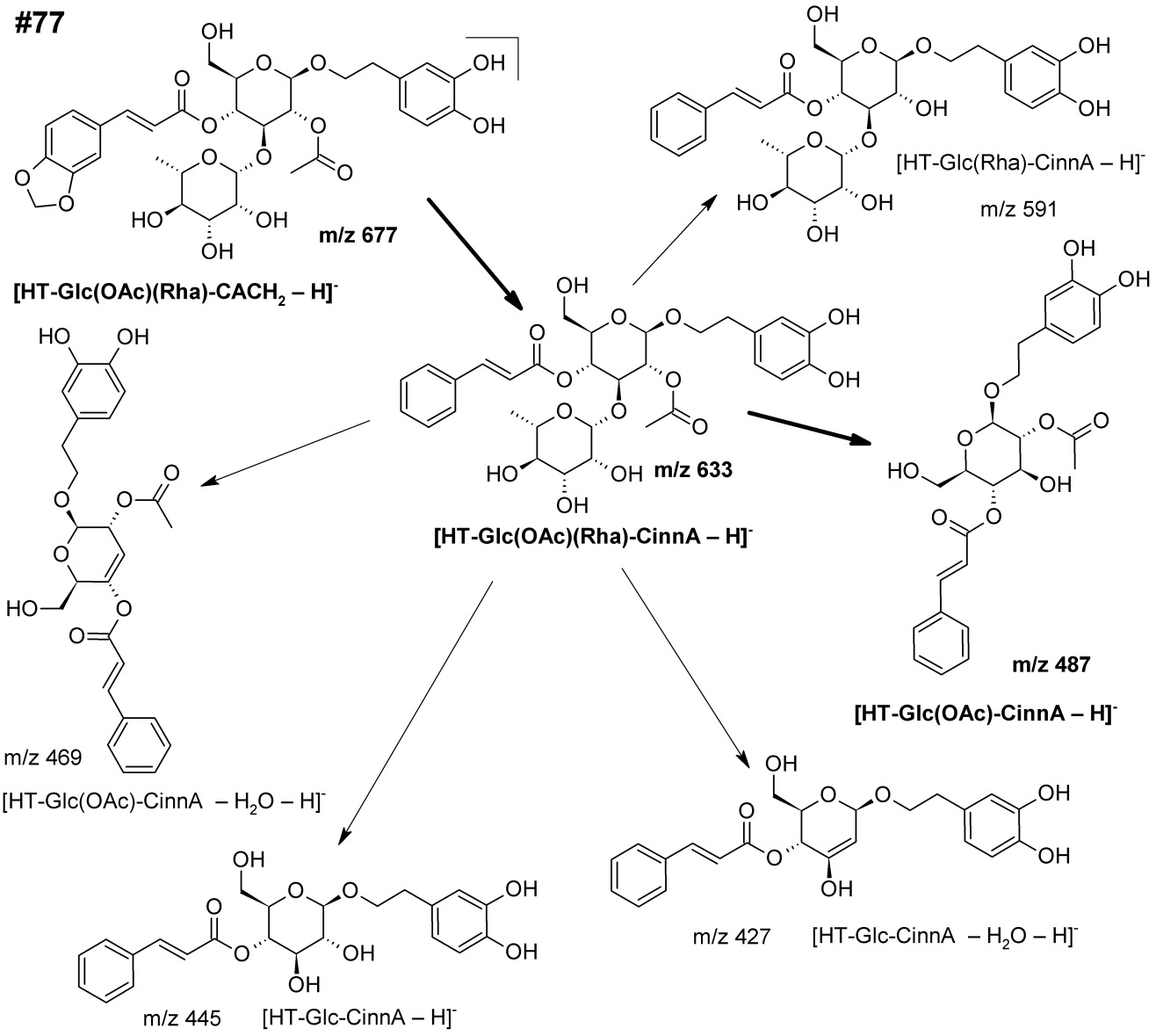

Supplementary Figure 6. Proposed fragmentation pattern of **#77**, identified as methylene-acetyl-acteoside. This natural product is one of the phenylethanoid glycosides of the *P. lanceolata* callus extract detected by negative mode LC-ESI-MS^3. The main fragmentation route is highlighted with bold arrows and bold font.

Supplementary Table 1. Results of statistical tests for effects of N source composition on the abundance of individual metabolites, quantified by LC-ESI-MS analysis of *P. lanceolata* calli grown on media with different N source compositions. NPs were ordered according to their retention times in LC.

No.	Rt	[M-H]$^-$	Cluster No.[a]	ANOVA *p* value				Fold change		Highest yield medium[f]
				N source[b]		NH_4^+/NO_3^- ratio[c]		vs MSM[d]	vs 20(0)[e]	
1	2.42	461	6	1.103E-02		7.590E-03		1.08	7.19	10(0.33)
2	2.51	683	4	1.614E-11	***	7.868E-01		2.77	2.57	10(0.33)
3	2.96	461	4	2.252E-03		5.832E-01		5.26	2.09	10(0)
4	3.93	683	6	3.260E-02		2.383E-02		2.10	49.96	10(0.33)
5	3.94	637	6	7.054E-03		4.453E-01		2.34	5.37	40(0.33)
6	4.46	655	3	2.202E-12	***	2.912E-03		3.30	6.04	10(0.33)
7	4.68	655	3	2.512E-10	***	4.223E-03		3.04	5.72	10(0.33)
8	4.85	801	3	7.659E-06	**	2.892E-02		1.88	14.56	10(0.33)
9	5.21	801	3	2.559E-07	***	1.245E-02		2.76	9.88	10(0.33)
10	6.86	755	6	1.717E-02		1.706E-01		1.02	2.32	60(0.25)
11	6.92	677	3	2.098E-01		5.571E-01		4.19	1.75	10(0.33)
12	6.92	801	3	3.116E-12	***	1.726E-02		4.16	4.97	10(0.33)
13	7.15	461	3	3.597E-03		5.974E-02		2.84	1.87	10(0)
14	7.43	677	3	3.075E-02		1.739E-01		1.37	1.16	40(0.33)
15	7.45	755	6	1.237E-07	***	1.360E-04		5.53	2.42	20(0.33)
16	7.49	683	6	1.564E-06	***	3.183E-02		5.45	1.04	20(0.33)
17	7.65	461	3	2.509E-03		1.099E-02		3.21	2.15	10(0)
18	8.08	639	4	6.318E-07	***	2.587E-02		1.84	1.92	10(0.33)
19	8.16	755	6	1.603E-03		1.135E-03		1.11	4.52	40(0.25)
20	8.41	637	1	1.355E-06	***	1.409E-05	**	23.88	1.84	10(0)
21	8.89	769	6	4.182E-03		1.313E-03		1.20	4.96	40(0.25)
22	9.07	477	1	1.552E-04		5.315E-03		2.00	1.37	10(0)
23	9.14	755	6	1.056E-02		1.856E-03		1.32	9.50	40(0.25)
24	9.24	655	5	3.382E-05	*	5.099E-02		1.63	2.39	10(0.33)
25	9.25	653	5	6.964E-02		2.988E-03		1.21	1.71	10(0.33)
26	9.30	677	2	1.135E-03		2.949E-05	*	1.76	1.15	10(0)
27	9.31	623	6	7.014E-02		2.292E-01		1.24	2.39	40(0.33)
28	9.35	637	1	1.082E-04	*	1.178E-05	**	6.05	1.90	10(0)
29	9.43	769	2	3.806E-04		2.054E-01		1.70	2.59	60(0.11)

30	9.61	477	1	2.112E-02		1.862E-04		1.86	1.24	40(0)
31	9.65	769	6	1.006E-03		7.710E-05	*	1.34	34.67	40(0.25)
32	9.67	653	5	1.689E-05	**	2.291E-02		1.46	2.05	10(0.33)
33	9.68	699	5	2.166E-05	**	3.350E-02		1.75	2.25	10(0.33)
34	9.69	655	5	4.605E-07	***	1.424E-01		2.62	3.84	10(0.33)
35	9.73	693	5	1.439E-02		2.752E-02		2.52	2.72	10(0.33)
36	9.80	637	1	4.275E-06	**	2.134E-05	**	4.32	1.71	10(0)
37	9.88	639	4	3.039E-06	**	4.825E-02		3.85	2.34	10(0)
38	9.99	653	4	4.827E-08	***	1.524E-02		2.58	2.86	10(0.33)
39	10.13	477	1	1.047E-03		1.375E-03		1.97	1.34	40(0)
40	10.15	677	2	3.693E-04		1.225E-05	**	1.95	1.24	10(0)
41	10.26	653	2	7.799E-06	**	1.834E-03		1.59	1.39	10(0)
42	10.27	655	2	2.256E-07	***	2.162E-03		2.35	1.81	10(0)
43	10.45	623	6	9.738E-02		1.724E-01		1.25	3.06	40(0.33)
44	10.47	477	1	2.800E-01		7.953E-04		2.10	1.36	40(0)
45	10.49	653	4	6.023E-12	***	6.207E-02		1.78	1.96	10(0.33)
46	10.49	655	4	4.853E-10	***	1.307E-02		3.61	2.29	10(0)
47	10.49	693	1	3.668E-01		3.867E-01		16.30	14.57	40(0)
48	10.49	699	2	7.226E-07	***	7.335E-03		1.96	1.59	10(0)
49	10.54	639	2	3.183E-11	***	4.255E-08	***	2.36	1.77	10(0)
50	10.66	709	4	3.132E-05	*	7.489E-01		2.28	1.72	10(0.33)
51	10.69	653	4	6.337E-04		6.961E-01		4.17	3.07	10(0.33)
52	10.95	709	4	7.406E-07	***	4.132E-01		2.77	1.66	10(0.33)
53	11.00	653	4	5.688E-15	***	4.123E-01		3.35	2.77	10(0.33)
54	11.01	655	4	4.616E-15	***	3.680E-01		6.66	4.27	10(0.33)
55	11.03	637	2	1.881E-03		5.133E-01		1.33	1.64	10(0.33)
56	11.19	709	2	7.083E-06	**	1.089E-01		3.25	1.76	10(0.33)
57	11.38	683	4	9.377E-09	***	5.337E-01		3.43	2.95	10(0.33)
58	11.49	461	4	9.970E-04		6.414E-01		2.15	2.05	10(0.33)
59	11.63	637	2	2.397E-03		2.884E-02		1.59	1.40	10(0)
60	11.68	667	6	2.723E-02		3.941E-01		1.27	4.62	60(0.11)
61	11.84	653	2	1.341E-05	**	3.610E-04		2.71	1.66	10(0)
62	11.87	699	4	1.030E-05	**	2.908E-01		4.64	3.13	10(0.33)
63	11.89	655	2	5.468E-08	***	1.935E-04		6.85	3.10	10(0)
64	11.97	667	5	3.844E-03		4.469E-02		1.26	1.80	40(0.25)
65	12.30	693	4	2.911E-05	*	1.221E-01		2.55	2.04	10(0.33)

66	12.33	653	2	1.171E-03		1.912E-02		1.91	1.69	60(0)
67	12.43	667	5	1.601E-03		4.851E-02		1.33	1.73	10(0.33)
68	12.45	461	4	2.324E-02		6.727E-01		2.43	2.14	10(0)
69	12.54	637	2	5.114E-08	***	1.567E-06	***	3.48	1.63	10(0)
70	12.54	723	2	7.125E-02		1.168E-01		3.75	1.46	10(0.33)
71	12.64	693	4	2.276E-10	***	8.303E-01		2.90	2.11	10(0.33)
72	12.96	693	4	9.950E-03		2.983E-01		6.71	2.92	10(0.11)
73	12.97	723	2	1.266E-04		1.634E-01		2.82	1.87	10(0.33)
74	13.04	653	2	5.073E-03		1.312E-05	**	4.28	1.83	10(0)
75	13.83	653	2	3.190E-05	*	2.612E-02		2.33	2.20	10(0)
76	13.86	699	2	4.545E-03		2.379E-01		2.50	2.36	10(0.33)
77	13.98	677	4	2.135E-05	**	3.591E-01		2.28	2.29	10(0.11)
78	14.30	653	2	2.142E-08	***	1.085E-03		1.56	1.85	10(0.33)
79	14.33	667	5	1.439E-02		5.204E-01		1.49	1.82	60(0.11)
80	14.33	677	4	2.087E-01		9.394E-01		1.57	1.92	10(0.33)
81	15.12	667	5	4.111E-02		4.039E-01		1.52	1.94	60(0.11)
82	15.37	637	3	8.294E-08	***	2.199E-01		4.69	9.64	10(0.33)
83	15.89	637	3	1.320E-10	***	8.909E-02		4.15	4.84	10(0.33)
84	16.85	677	3	1.254E-03		1.744E-01		3.66	3.48	10(0.25)
85	16.93	693	6	3.048E-02		7.882E-04		1.40	7.08	40(0.33)
86	17.27	677	3	8.615E-05	*	1.101E-01		2.36	2.12	10(0.33)
87	17.85	693	6	3.977E-02		3.027E-04		1.41	10.36	40(0.33)
88	19.22	709	1	8.514E-01		3.901E-02		5.18	2.12	20(0.11)
89	19.23	699	1	1.883E-01		1.063E-06	***	3.57	1.40	40(0)

The significance levels *, $p < 0.00011$; **, $p < 2.25e\text{-}4$; ***, $p < 2.25e\text{-}5$ were used (Bonferroni correction, see 4.9.). Abbreviations: MSM, Murashige Skoog medium, 60(0.33); Rt, retention time. Notes: [a]., Cluster according to hierarchical cluster analysis of scaled abundance data. See text and Fig.4.b. for details. [b]., *p* value results of ANOVA to test the effect of the total N source concentration on the abundance of individual metabolites. [c]., *p* value results of ANOVA to test the effect of the NH_4^+ / NO_3^- ratio concentration on the abundance of individual metabolites. [d]., The NP abundance of the calli grown on the medium with best yield was compared to the original Murashige Skoog medium, 60 mM total N source (Murashige and Skoog, 1962), 1:2 NH_4^+ / NO_3^- ratio, abbreviated 60(0.33); [e]., The NP abundance of the calli grown on the medium with best yield was compared to the medium described in (Budzianowska et al., 2004) for cultivation of *P. lanceolata* calli: 20 mM total N source, only NO_3^-,

abbreviated 20(0); [f]., N source composition of the medium that yielded the highest mean concentration (abundance / mg dry wt.) for a given metabolite. Total N concentration (mM) is followed by the ratio of NH_4^+ in the total N source, in parentheses.

Supplementary Table 2. Results of the *in silico* yield optimization experiment for individual NPs. Columns: FF, best medium for yield of a given NP as obtained by the full-factorial experimental design. OFAT #1-4: best media for yield of a given NP as obtained by the different virtual OFAT designs. Only suboptimal NP yields are presented. The yield advantage of the best medium from the FF strategy is shown as fold increase compared to the abundance of the suboptimal result from the virtual OFAT optimization. Strategies: #1: starting from MSM, NH_4^+/NO_3^- ratio optimized first; #2: starting from 20(0), NH_4^+/NO_3^- ratio optimized first; #3: starting from MSM, N source concentration optimized first; #4:starting from 20(0), N source concentration optimized first.

No.	FF	OFAT #1	fold	OFAT #2	fold	OFAT #3	fold	OFAT #4	fold
1	10(0.33)			60(0.25)	1.51				
2	10(0.33)	10(0.11)	1.24	10(0)	1.02				
3	10(0)	10(0.11)	1.87			40(0.33)	1.62		
4	10(0.33)			10(0.25)	1.50			60(0.33)	2.10
5	40(0.33)	60(0.11)	1.52	60(0)	2.40			60(0.11)	1.52
6	10(0.33)								
7	10(0.33)								
8	10(0.33)								
9	10(0.33)			10(0)	2.65				
10	60(0.25)			60(0.33)	1.02			10(0.33)	1.53
11	10(0.33)	10(0.11)	1.70	20(0.25)	1.04				
12	10(0.33)	10(0)	1.50	10(0)	1.50				
13	10(0)	60(0.11)	1.08						
14	40(0.33)	60(0.11)	1.27	20(0)	1.16			20(0)	1.16
15	20(0.33)								
16	20(0.33)	20(0)	1.04						
17	10(0)								
18	10(0.33)								
19	40(0.25)	60(0.11)	1.06			60(0.11)	1.06	60(0.11)	1.06
20	10(0)								
21	40(0.25)	60(0.11)	1.19			60(0.11)	1.19	60(0.11)	1.19
22	10(0)	10(0.11)	1.23						
23	40(0.25)	60(0.11)	1.10			60(0.11)	1.10	60(0.11)	1.10
24	10(0.33)	60(0.11)	1.49	10(0)	1.48				
25	10(0.33)	60(0.11)	1.18					40(0.25)	1.10
26	10(0)								
27	40(0.33)	60(0.25)	1.17	60(0.11)	1.18			10(0.11)	1.38
28	10(0)								
29	60(0.11)					10(0.11)	1.22		
30	40(0)					10(0)	1.22		
31	40(0.25)	60(0.33)	1.34			60(0.33)	1.34	60(0.33)	1.34
32	10(0.33)	60(0.11)	1.45						
33	10(0.33)	10(0.11)	1.64	10(0)	1.37				
34	10(0.33)	10(0.11)	2.02	10(0)	1.45				
35	10(0.33)	40(0.25)	1.42	10(0)	1.82				
36	10(0)								

37	10(0)								
38	10(0.33)			10(0)	1.13				
39	40(0)	10(0.11)	1.22						
40	10(0)								
41	10(0)	10(0.11)	1.21						
42	10(0)								
43	40(0.33)	60(0.25)	1.24	10(0.11)	1.25			10(0.11)	1.25
44	40(0)					10(0)	1.53		
45	10(0.33)	10(0.11)	1.15	10(0)	1.07				
46	10(0)	10(0.11)	1.41						
47	40(0)	60(0.11)	12.54						
48	10(0)	10(0.11)	1.35						
49	10(0)								
50	10(0.33)	10(0.11)	1.15	10(0)	1.19				
51	10(0.33)	60(0.11)	1.05	40(0.25)	1.66				
52	10(0.33)	10(0.11)	1.16	10(0)	1.08				
53	10(0.33)	10(0.11)	1.14	10(0)	1.04				
54	10(0.33)	10(0.11)	1.20	10(0)	1.07				
55	10(0.33)	60(0.11)	1.01	10(0)	1.05				
56	10(0.33)	10(0.11)	1.44	10(0)	1.27				
57	10(0.33)	10(0.11)	1.43	10(0)	1.11				
58	10(0.33)	10(0.11)	1.26	10(0)	1.06				
59	10(0)	60(0.11)	1.09						
60	60(0.11)			40(0.25)	1.26			10(0.33)	1.41
61	10(0)								
62	10(0.33)	10(0.11)	1.64	10(0)	1.15				
63	10(0)								
64	40(0.25)	60(0.11)	1.14	40(0.33)	1.03			60(0.11)	1.14
65	10(0.33)	10(0.11)	1.10	40(0)	1.03			40(0)	1.03
66	60(0)					10(0)	1.08		
67	10(0.33)	60(0.11)	1.22	10(0)	1.39				
68	10(0)	60(0.11)	1.30						
69	10(0)								
70	10(0.33)	60(0.11)	1.15	10(0)	1.12				
71	10(0.33)	10(0.11)	1.14	10(0)	1.12				
72	10(0.11)			10(0)	1.36				
73	10(0.33)	10(0.11)	1.51	10(0)	1.23				
74	10(0)								
75	10(0)								
76	10(0.33)	40(0)	1.15	40(0)	1.15			40(0)	1.15
77	10(0.11)			10(0.33)	1.12				
78	10(0.33)	10(0)	1.06	10(0)	1.06				
79	60(0.11)			10(0)	1.01	40(0.25)	1.12	10(0)	1.01
80	10(0.33)	10(0)	1.15						
81	60(0.11)			40(0.33)	1.13	40(0.33)	1.13		
82	10(0.33)	10(0.11)	2.73	10(0)	1.24				
83	10(0.33)	10(0.11)	2.10	10(0)	1.04				
84	10(0.25)	10(0)	2.33	10(0)	2.33				
85	40(0.33)							10(0.33)	2.07
86	10(0.33)	10(0.11)	1.76	10(0)	1.19				

87	40(0.33)							10(0.33)	2.34
88	20(0.11)	40(0)	1.16			10(0)	1.75	40(0)	1.16
89	40(0)								